GAMMA DOSE RATE IMPROVEMENT IN GASES BY ELECTRON-CONVERSION PLATES

A Thesis

Submitted to the Graduate Faculty of the
Louisiana State University and
Agriculatural and Mechanical College
in partial fulfillment of the
requirements for the degree of

Master of Science

in

The Department of Nuclear Engineering

by

Sudesh K. Mahajan
BS, Kurukshetra University, India, 1970

August 1974

Dedicated to

my parents

ACKNOWLEDGMENT

The author wishes to acknowledge the expert advise and guidance of Dr. Robert C. McIlhenny without which this presentation would not have been possible. The author also wishes to express his sincere appreciation to Drs. John C. Courtney, Frank A. Iddings and Myron H. Young for their helpful suggestions for this presentation.

Also thanks is given to Carol A. Kinchen for typing of this thesis.

To these and many others who have helped make this project possible, the author wishes to express his appreciation.

TABLE OF CONTENTS

LIST OF TABLES

LIST OF FIGURES

LIST OF FIGURES (CONT'D.)

ABSTRACT

Although gamma radiolysis is employed for several important industrial processes, energy transfer from a gamma field to a gas phase system is inefficient. Energy transfer could potentially be improved, however, by taking advantage of metal plates introduced into the reaction vessel to provide an electron flux superimposed on the gamma field. This possibility was evaluated through a simple model in which monoenergetic, monodirectional gamma radiation is incident upon a pair of infinite-plane parallel plates defining the gas volume. Plate thickness was selected as one-half the range of the average-energy electrons generated by photoelastic and Compton-scatter processes, assuming a linear electron-attenuation approximation. Inter-plate distance was obtained through the Spencer-Attix cavity-ionization-chamber theory by calculating gas/wall stopping power ratios, and selecting the distance at which electron-derived ionization density becomes essentially constant. For aluminum as the plate material, and air as the target gas, half-range plate thickness were calculated by a straightforward Fortran IV program to be 0.13mm for cesium-137, and 0.45mm for cobalt-60 gamma sources. Inter-plate spacing for both sources was selected from calculated values to be 10mm. The ratio of gamma-plus-electron dose rate to gamma dose rate alone was calculated for both sources to be 2.1 for the conditions specified. Application of the electron-conversion plate technique for increasing energy transfer is considered to be practical in a multiplate array of

either concentric cylinders or close-packed hexagonal cross-section tubes in a right-cylindrical irradiation vessel exposed to an external annular source.

CHAPTER I

INTRODUCTION

The controlled release of nuclear energy and the accompanying release of nuclear radiation has focused a good deal of attention on the possible use of such radiations in the chemical industry. Radiation may be used to bring about many different types of chemical change. Irradiation of various gases or mixture of gases has been investigated to produce new products.

For example, irradiation of hydrocarbons, such as methane and ethylene, has been extensively studied and has been used to produce higher hydrocarbons and polymers.[1] Ethyl bromide can be synthesized with 99.5% purity by irradiating a mixture of ethylene and hydrogen bromide; at room temperature, the radiolytic yield (product molecules formed per 100 ev of radiation absorbed) in this case is about 100,000.[2]

The sources of radiation used in radiation-chemical studies are both radioactive isotopes and a variety of particle accelerators. More recently spent fuel rods from a nuclear reactor have also been considered as a possible source of radiation. But artificial radioactive isotopes such as cobalt-60, cesium-137 and strontium-90 are most commonly used. Both cobalt-60 and cesium-137 are gamma sources, and strontium-90 is a pure beta emitter.

Gamma radiation is electromagnetic radiation that is produced by nuclear rearrangements. The wave length of gamma radiation is many orders of magnitude shorter than that of visible radiation.

Primary interactions of gamma rays with matter involve the production of energetic secondary electrons. It is the interaction of these secondary electrons with matter that deposit most of the energy in any absorbing material, usually through ionization or excitation of its atoms. If this absorber is solid or liquid, there are enough atoms of the absorber available for efficient interaction of gammas with them to produce secondary electrons. But for gases, where the density is much lower, not enough atoms of the absorber are available for efficient electron production. It may be advantageous, however, to utilize the secondary electrons produced in the walls of a container (reaction vessel) to increase the dose rate for materials in the gaseous phase.

The optimum thickness of the wall would be that for which the maximum number of secondary electrons produced within the wall would escape from the wall.

Theoretically, there are twelve different mechanisms, for the interaction of photons with matter.[3] Fortunately, the most important processes in the gamma energy range of interest are the photoelectric and Compton effects. The partial probabilities for photon interaction in any one of the possible ways is a function of photon energy and the composition of the interacting material. Since interactions do not always occur, the photon may pass through the wall, but since the interactions are statistical in nature, there will always be a finite probability of interaction with any medium.

The secondary electrons will lose their energy by inelastic collisions with atomic electrons or nuclei, and by elastic collisions

with atomic electrons or nuclei, depending upon initial kinetic energy, but they will travel well defined distances before losing all of their kinetic energy. This distance is called path length. The mean path length of many monoenergetic electrons is called the range. The range of an electron is a material is directly proportional to the energy of the electron and inversely proportional to the density of the material. Low atomic number (Z) materials will allow a maximum number of electrons to escape from the walls of the container. Glass, polythylene, and aluminum are a few examples of low Z material which may be attractive. Aluminum is a more suitable material because there is no gamma radiation damage in a metal as compared to polyethylene and glass.

The distance between two walls will be optimum when this is within the range in gas of a maximum number of electrons escaping from the wall. The effects of secondary electrons produced in the walls of the container have been reported earlier for several cases. In the case of Fricke dosimeter, for example, J. Weiss found that for identical exposures to Co-60 the concentration of Fe^{3+} was greater when reaction vessel diameters up to 10mm were used, and was constant for diameters greater than 10mm.[4] The use of lead filters in photographic films used in radiography is an example of the utilization of secondary electrons.[5]

The purpose of this thesis is to investigate theoretically the increase in energy transfer from gamma to gas phase for an optimum thickness of the wall of a container, the distance between two walls, and the Z of the wall material.

CHAPTER II

INTERACTION OF GAMMA RADIATION AND ELECTRONS WITH MATTER

There are twelve possible interactions of gamma with matter.[3] Some of these interactions have never been observed, and most of the rest occur infrequently. Three of these interactions cover adequately the energy range of 0.01 to 10 Mev. These are:

1. Photoeletric Interaction
2. Compton Interaction
3. Pair Production

Pair production is the dominant mode of interaction of photons above 10 Mev with all matter. Other interactions, like photonuclear reactions, photofission, etc. take place infrequently. Figure 1 provides a handy guide to the relative importance of the three main interactions over a broad range of energies of incident photons and atomic numbers of the attenuating materials.

Photoelectric Interaction[6]

In photoelectric collisions the entire energy of the incident photon is absorbed by an atom of the medium. There is no scattered residual photon. The attenuation of the primary radiation is due to complete absorption of the energy of the incident photon. One electron, usually from the K or L shell, is then immediately ejected with kinetic energy T such that

$$T = h\nu - B_e \qquad (1)$$

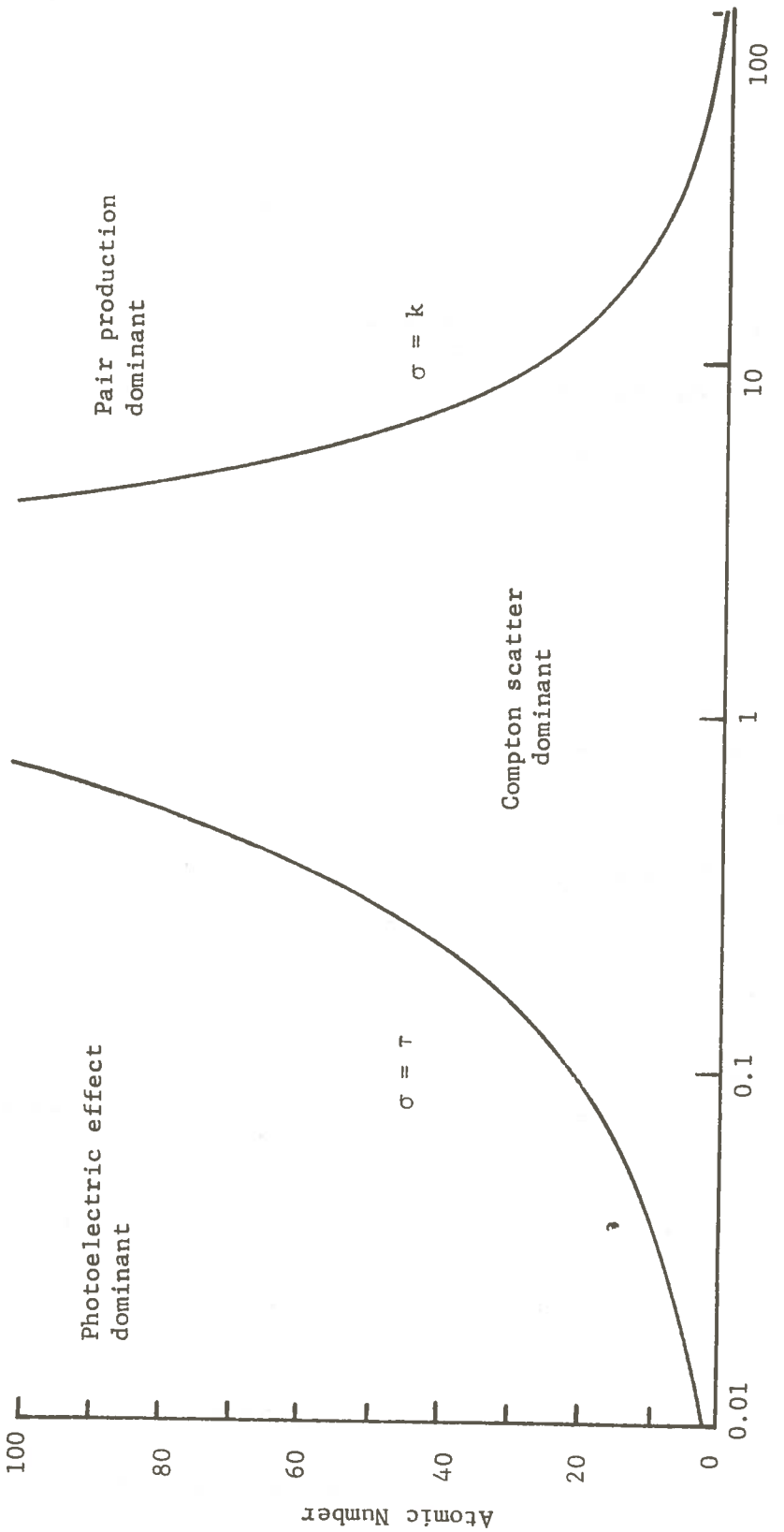

Figure 1: Relative Importance of Major Absorption Processes with Respect to Photon Energy and Atomic Number of the Absorber[7]

where

$h\nu$ = Primary photon energy

B_e = Binding energy of the electron before being ejected from the atom

Momentum is conserved by the backward recoil of the entire residual atom. Electrons will move in a forward direction (direction of the primary radiation. Let τ_a be the probability of photoelectic interaction in units of cm^2/atom, then[8]

$$\tau_a \simeq K. \frac{Z^4}{(h\nu)^3} \qquad (2)$$

K = constant

Z = atomic number

The binding energy of K shell electrons for Pb = 88.0 Kev. There is no single closed formula describing τ_a accurately over a wide range of $h\nu$. The above formula is approximate, but is useful in our case. Now,

$$\tau = N. \tau_a$$

where

τ = linear attentuation coefficient for photoelectric interactions

N = atoms per cm^3

The units of τ are (cm^{-1}).

If ρ = density (gm/cm^3) then,

$\frac{\tau}{\rho}$ = mass attenuation coefficient and has dimensions of square centimeter per gram.

Experimental and theoretical values of linear attentuation coefficients for Al, Pb, etc., are provided by several authors.[9] For any other material approximate value can be found by:

$$\left(\tau_1/\tau_2\right) = \left(\rho_1/\rho_2\right)\left(A_2/A_1\right)\left(Z_1/Z_2\right)^n \qquad (3)$$

A = atomic weight

Z = atomic number

ρ = density

n = constant whose value varies from 4.0 to 4.6

Values for n for various γ energies are presented in Figure 2.

Direction of Electron

At low photon energies, the photoelectrons tend to be ejected at a right angle to the direction of incidence. At higher energies, as in our case, the angular distribution is more in the forward direction. Figure 3 shows the theoretical values for directional distribution of photoelectrons per unit of solid angle as calculated by Davisson.[10] It is clear from the figure that in the case of Co-60 the highest number of photoelectrons make an angle of 15^{o} with the direction of γ rays, and in the case of Cs-137 that the angle is 20^{o}.

Compton Interaction[11]

In the Compton interaction, a photon interacts with an electron which may be loosely bound or free, so that the electron is accelerated and the photon is deflected with reduced energy. This is satisfactory for photon energies so large compared with the electron binding

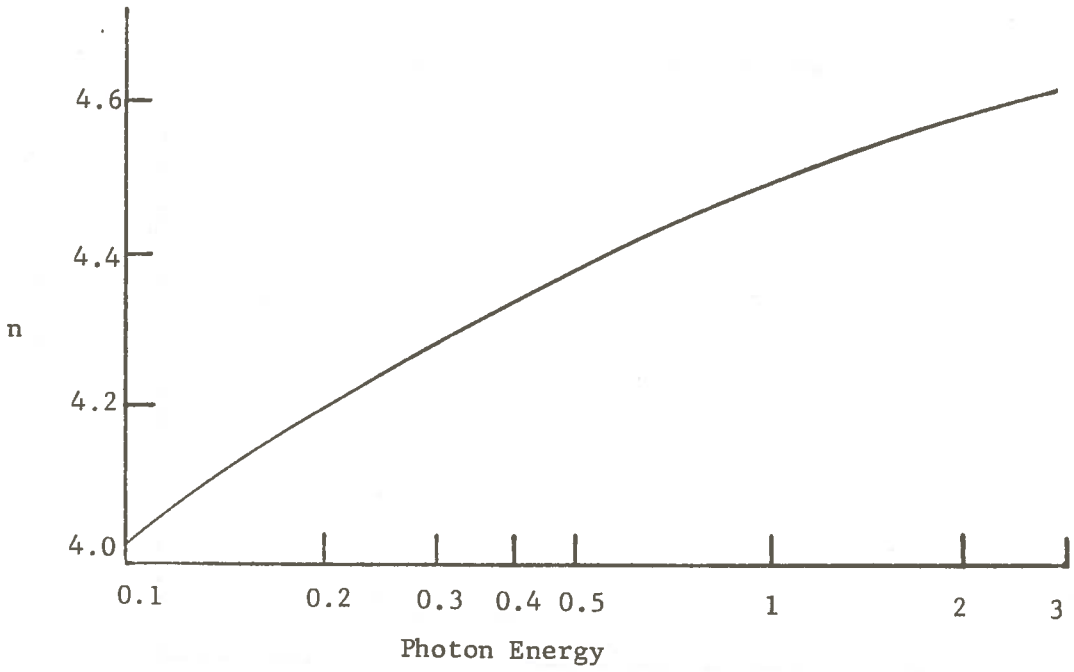

Figure 2: Energy Dependence of the Index for Photoelectric Attenuation Coefficient Calculation[9]

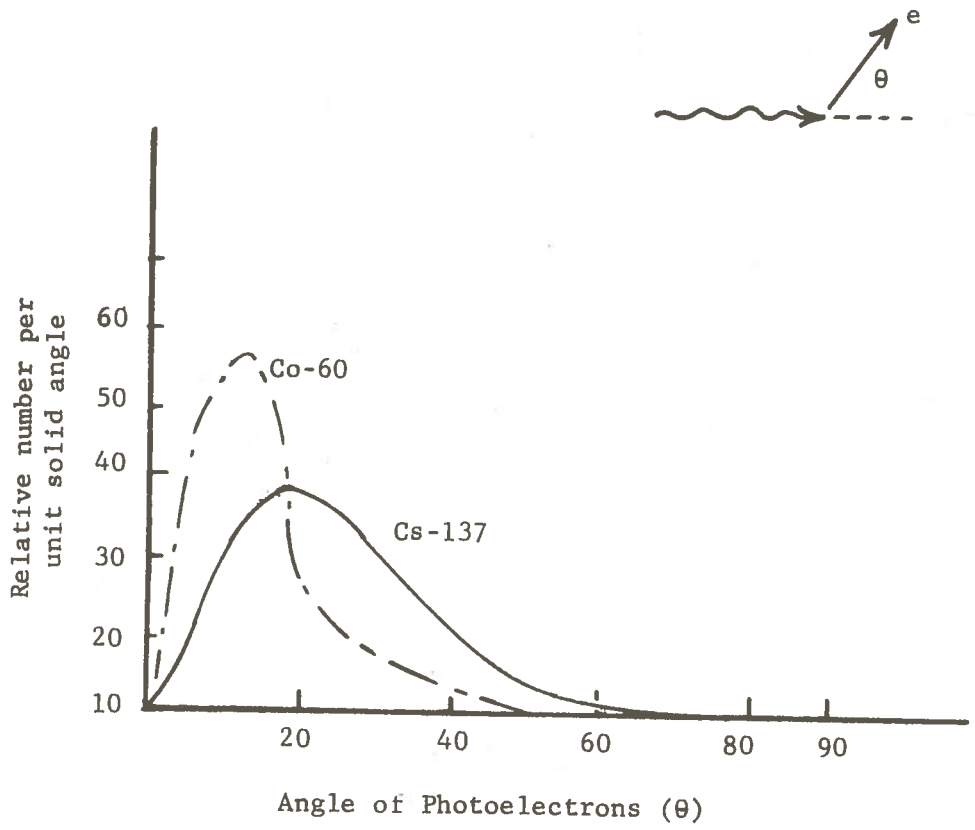

Figure 3: Directional Distribution of Photoelectrons per Unit Solid Angle.[10]

energies that the electrons can be considered free. Figure 4 shows the interaction of a single photon with the struck atom. Let the Compton electron make an angle Φ with the direction of incidence, and the scattered photon make an angle of θ with the direction of incidence. Let $h\nu_o$ ahd $h\nu$ be the incident and scattered photon energies respectively, and let T be the energy of the Compton electron. From the law of conservation of energy it is seen that the electron has acquired a kinetic energy that is equal to the energy difference of the incident and the deflected photon. Therefore,

$$h\nu_o - h\nu = T \tag{4}$$

The incident energy can be written in terms of the dimensionless quantity

$$\alpha = \frac{h\nu_o}{m_o c^2} \tag{5}$$

where

m_o = rest mass of the struck electron

c = velocity of light

actually

$m_o c^2 = 0.51$ Mev.

Then the conservation laws gives, for the energy of a Compton scattered electron,

$$T = h\nu_o \frac{\alpha\,(1-\cos\theta)}{1 + \alpha\,(1-\cos\theta)} \tag{6}$$

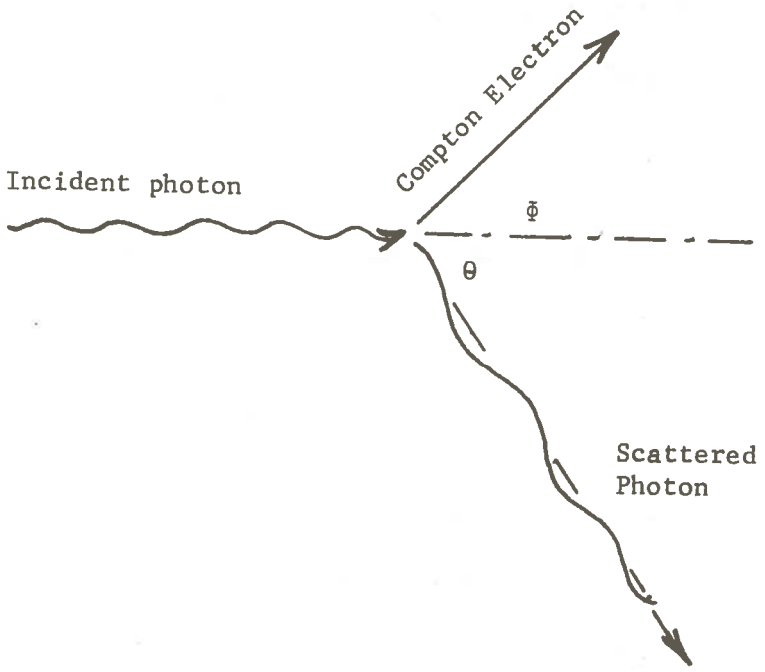

Figure 4: Diagram of the Compton Scatter Process

and

$$T_{max} = h\nu_o \frac{2\alpha}{1 + 2\alpha} \text{ for } \theta = 180^o$$

The angle Φ is related to the photon scattering angle θ, by[12]

$$\cot \Phi = (1 + \alpha) \tan \frac{\theta}{2} \tag{7}$$

The probability of a photon being scattered with a definite energy or direction, and the probability of Compton interaction as a whole, were derived quantum mechanically by Klein and Nishina.[13] The Klein-Nishina formula for the total electronic Compton absorption coefficient is

$$e\sigma = 2\pi r_o^2 \left\{ \frac{1 + \alpha}{\alpha^2} \left[\frac{2(1 + \alpha)}{1 + 2\alpha} - \frac{\ell n\,(1 + 2\alpha)}{\alpha} \right] + \frac{\ell n\,(1 + 2\alpha)}{2\alpha} - \frac{1 + 3\alpha}{(1 + 2\alpha)^2} \right\} \text{ cm}^2/\text{electron} \tag{8}$$

where r_o is the classical radius of the electron (2.818×10^{-13} cm).

The fraction of the incident photon energy, per electron/cm^2, that the scattered photons retain is given by the Compton scattering coefficient $e\sigma_s$

$$e\sigma_s = \pi r_o^2 \left[\frac{\ell n\,(1 + 2\alpha)}{\alpha^3} + \frac{2(1 + 2)(2\alpha^2 - 2\alpha - 1)}{\alpha^2 (1 + 2\alpha)^2} + \frac{8\alpha^2}{3(1 + 2\alpha)^2} \right] \tag{9}$$

The fraction of the incident photon energy transferred to the recoil electrons, per electron/cm^2, is given by the energy Compton absorption coefficient, $e\sigma_a$

$$ {}_e\sigma_a = {}_e\sigma - {}_e\sigma_s \tag{10} $$

The Compton total linear attentuation coefficient σ is given by,

$$ \sigma = N.Z.\ {}_e\sigma\ \text{cm}^{-1} \tag{11} $$

If the value of σ for one material is known, σ for other materials can be calculated by[14]

$$ \sigma_1 = \sigma_2 \cdot \frac{\rho_1}{\rho_2} \cdot \frac{A_2}{A_1} \cdot \frac{Z_1}{Z_2} \tag{12} $$

where

ρ = density of the material

A = atomic weight of the material

Z = atomic number of the material

The average energy per Compton electron is therefore given by

$$ T_{av} = h\nu_o \frac{{}_e\sigma_a}{{}_e\sigma} \tag{13} $$

For $\alpha = 1$, that is $h\nu_o = 0.51$ Mev, ${}_e\sigma_a$ has a maximum value in a particular absorber.

Angular Distribution of Electrons[15]

The differential collision cross section, $d({}_e\sigma)/d\Omega$ for incident radiation (unpolarized beam) is given by

$$ \frac{d({}_e\sigma)}{d\Omega} = \frac{r_o^2}{2} \left(\frac{\nu'}{\nu_o}\right)^2 \left(\frac{\nu_o}{\nu'} + \frac{\nu'}{\nu_o} - \sin^2\theta\right) \tag{14} $$

where

$d\Omega$ = component of solid angle.

Now, the solid angle per unit angle = $d\Omega/d\theta = 2\pi \sin\theta$; hence,

$$\frac{d(e^{\sigma})}{d\theta} = \frac{r_o^2}{2}\left(\frac{\nu_o}{\nu'} + \frac{\nu'}{\nu_o} - \sin^2\theta\right)\left(\frac{\nu'}{\nu_o}\right)^2 \cdot 2\pi\sin\theta \qquad (15)$$

and the units of differential collision cross section are cm^2/electron. The above relation gives the number vs. angle distribution of scattered photons. The number vs. angle distribution of Compton electrons is given by

$$\frac{d(e^{\sigma})}{d\Phi} = \frac{d(e^{\sigma})}{d\Omega'} 2\pi\sin\Phi \qquad (16)$$

and

$$\frac{d\Omega}{d\Omega'} = -\frac{1}{1+\alpha}\frac{(1+\cos\theta)\sin\theta}{\sin^3\Phi} \qquad (17)$$

From Equations 14 and 17 we can find the following relationship,

$$\frac{d(e^{\sigma})}{d\Phi} = \frac{r_o^2}{2}\left(\frac{\nu_o}{\nu'} + \frac{\nu'}{\nu_o} - \sin^2\theta\right)\left(\frac{\nu'}{\nu_o}\right)^2 \cdot \left(\frac{-1}{1+\alpha} \cdot \frac{(1+\cos\theta)}{\sin^3\Phi}\sin\theta\right)$$

$$\cdot(2\pi \sin\Phi) \qquad (18)$$

Figure 5 shows the number vs. angle distribution of Compton electrons for various primary photon energies.

The energy spectrum of Compton electrons is given by:

$$\frac{d(e^{\sigma})}{dT} = \frac{d(e^{\sigma})}{d\Omega} \cdot \frac{2\pi}{\alpha^2 m_o c^2}\left[\frac{(1+\alpha)^2 - \alpha^2\cos^2\theta}{(1+\alpha)^2 - \alpha(2+\alpha)\cos^2\theta}\right] \qquad (19)$$

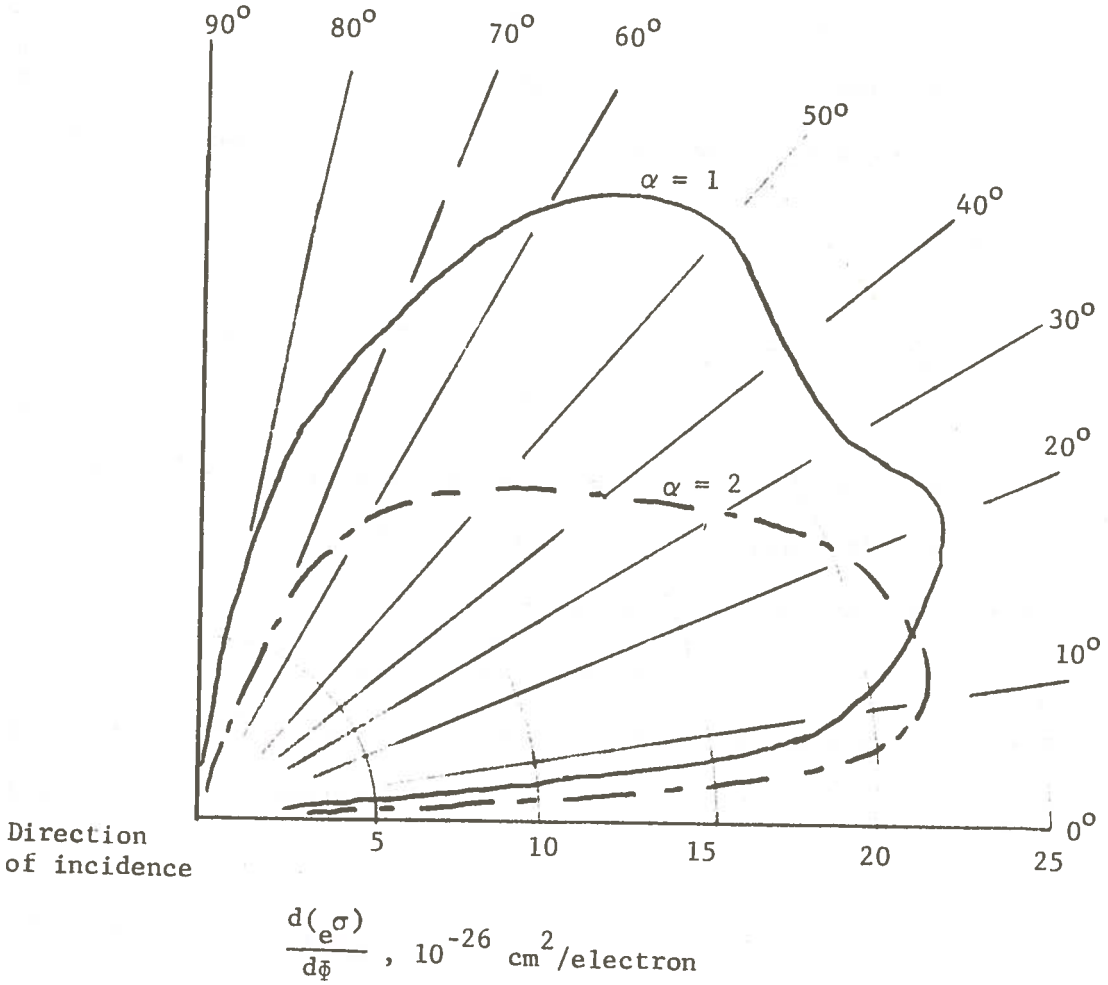

Figure 5: Number versus Angle Distribution for Compton Electrons.[15]

Figure 6 shows the energy distribution of Compton electrons produces by primary photons whose energies are 0.51 Mev and 1.2 Mev.

Pair Production[17]

Pair production is possible only for photon energies above 1.02 Mev. In this interaction, the photon is completely absorbed and in its place appears a positron-negatron pair whose total energy is equal to $h\nu$. Thus,

$$h\nu = (T_- + m_o c^2) + (T_+ - m_o c^2) \tag{20}$$

where

T_o and T_+ are kinetic energies of the negatron and positron, respectively, and $m_o c^2$ = 0.51 Mev. Thus it is clear that for cesium-137 ($h\nu$ = 0.6616 Mev) pair production is not possible; for Co-60 ($h\nu$ 1.33, 1.17 Mev) it is almost neglegible. The average positron receives a maximum of about 0.0075Z Mev more kinetic energy than the average negatron.

Interaction of Electrons with Matter[18]

The primary interaction of gamma rays with materials involves the production of energetic secondary electrons. Further interaction of these electrons with matter can be classified into four major divisions:

1. Inelastic collisions with atomic electrons
2. Inelastic collisions with atomic nuclei

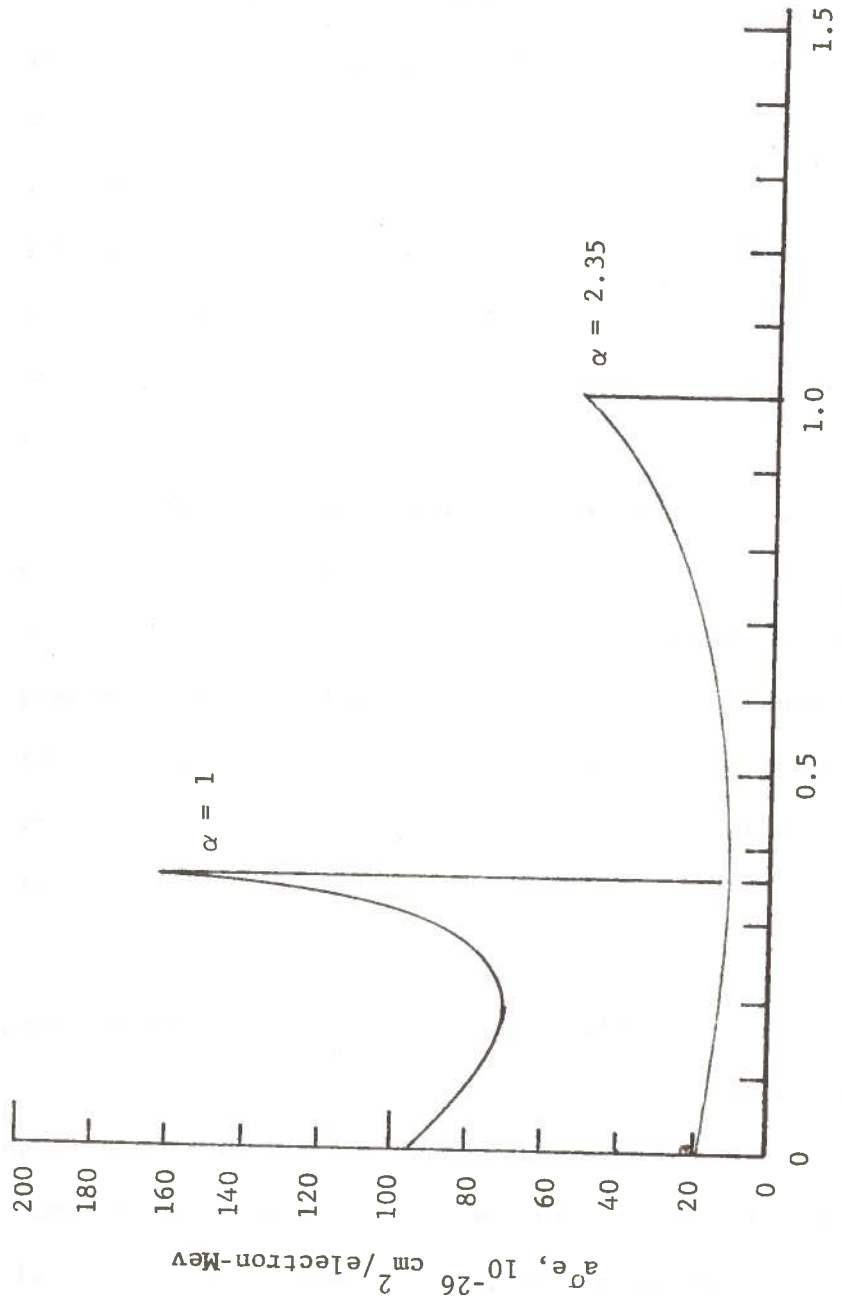

Figure 6: Energy Distribution of Compton Electrons For 0.51 Mev (α = 1) and 1.2 Mev (α = 2.35).

3. Elastic collisions with atomic nuclei

4. Elastic collisions with atomic electrons

Of the four possible interactions, only the first three are of any practical importance. Elastic collision with atomic electrons is only important for low-energy electrons, i.e., $T < 100$ ev. Inelastic collisions involve the transformation of kinetic energy into some other form of energy, such as ionization, excitation, or electromagnetic radiation. Elastic collisions involve the transfer of energy to another body; the energy however remains as kinetic energy.

The relative importance of these interactions varies strongly with the energy of the electrons and, to a smaller extent, with the nature of the interacting material; at high energies, energy is lost predominantly by radiation emission and at low energies through inelastic collisions. Elastic scattering with the nuclei is of greatest importance at low energies, i.e., in the low Mev range and for high atomic number materials.

Inelastic Collisions with Atomic Electrons

In this interaction, kinetic energy of electrons is transferred into some other form of energy such as excitation and ionization. Some of the atoms (or molecules) of the material are excited, that is, electrons are transferred from the ground state into an excited state. In the ionization process, one or more electrons are completely separated from an atom, leaving behind a positive ion. Most of the energy is taken by outgoing electrons and the recoil energy of the ion is very likely to be negligible.

This process is dominant for electron energies below those at which Bremsstrahlung emission occurs. The energy loss by electrons through inelastic collisions with atomic electrons, as derived by Bethe[19], is

$$-\left(\frac{dE}{dx}\right) = \frac{2\pi Ne^4 Z}{m_o v^2}\left[\ell n \frac{m_o v^2 E}{2I^2(1-\beta^2)} - (2\sqrt{1-\beta^2}-1+\beta^2)\,\ell n\, 2 + 1-\beta^2 + \frac{1}{8}\right.$$

$$\left.(1-\sqrt{1-\beta^2})\right]^2 \text{ergs/cm} \qquad (21)$$

where

v = velocity of the electron in cm/sec

$\beta = \frac{v}{c}$, c is velocity of light in cm/sec

I = mean excitation potential for the atoms of the material in ergs

N = number of atoms per cubic centimeters

e = charge of an electron in e.s.u.

m_o = rest mass of an electron in grams

Z = atomic number of the material

$-\left(\frac{dE}{dx}\right)$ = the energy loss per unit path, is known as the specific energy loss or stopping power S.

If S_m is the mass stopping power then

$$S_m = -\left(\frac{dE}{dx}\right) \times \frac{1}{\rho} \text{ ergs cm}^2/\text{gram}$$

where ρ is the density of the material.

Inelastic Collisions with Atomic Nuclei[18]

High speed electrons passing close to the nucleus of an atom undergo a deceleration. When an electron undergoes deceleration, it emits electromagnetic radiation with an amplitude proportional to the acceleration. This is called Bremsstrahlung. For electrons, Bremsstrahlung is negligible below 100 Kev but becomes the predominant mode of energy loss at an electron energy between 10 and 100 Mev (the energy depends on stopping material). It is greatest for high atomic number materials. A critical energy T_c can be defined at which energy loss due to electron collisions is equal to the loss due to Bremsstrahlung; approximately,[20]

$$T_c = \left[\frac{700}{(Z + 1.2)}\right] \text{Mev} \tag{22}$$

For aluminum T_c = 50 Mev, and for lead T_c is about 8.4 Mev. An estimate of the ratio r, of the energy loss due to Bremsstrahlung to that due to collision is given by[20]

$$r \approx \frac{TZ}{700} \tag{23}$$

This ratio r in the case of aluminum for 1 Mev electrons is approximately 0.018, i.e., the energy loss due to Bremsstrahlung is about two percent of the energy loss due to excitation and ionization. For this thesis inelastic collision with atomic nuclei is almost negligible.

CHAPTER III

DEVELOPMENT OF THE MODEL

As stated in Chapter I, the objective of this thesis is to develop a model to allow evaluation of the possibility that incorporation of electron conversion plates in a reaction vessel can increase the energy deposition rate in a gas phase during gamma radiolysis, and to estimate optimum plate thickness and inter-plate spacing. Certain assumptions must be made to establish a model amenable to calculation, including

A. Suitable geometry

B. Incident gamma energy

C. Target gas

D. Appropriate output parameter

E. Wall material

The geometrical arrangement of a practical irradiator, such as a cylindrical vessel surrounded by a annular radiation source as shown in Figure 7, imposes calculational difficulties with regard to gamma field uniformity, gamma spectrum, and angle of incidence. These difficulties are non-contributory to the fundamental question to be answered, although they would have to be included for detailed calculations subject to experimental verification. If a cylindrical geometry is extended infinitely in the axial direction, and the radius is extended to infinity, the result is that of infinite plane parallel plate geometry with the radiation incident from one direction. Then if the source is removed to infinity, the radiation can be considered as monodirectional. This geometry has been assumed for the model.

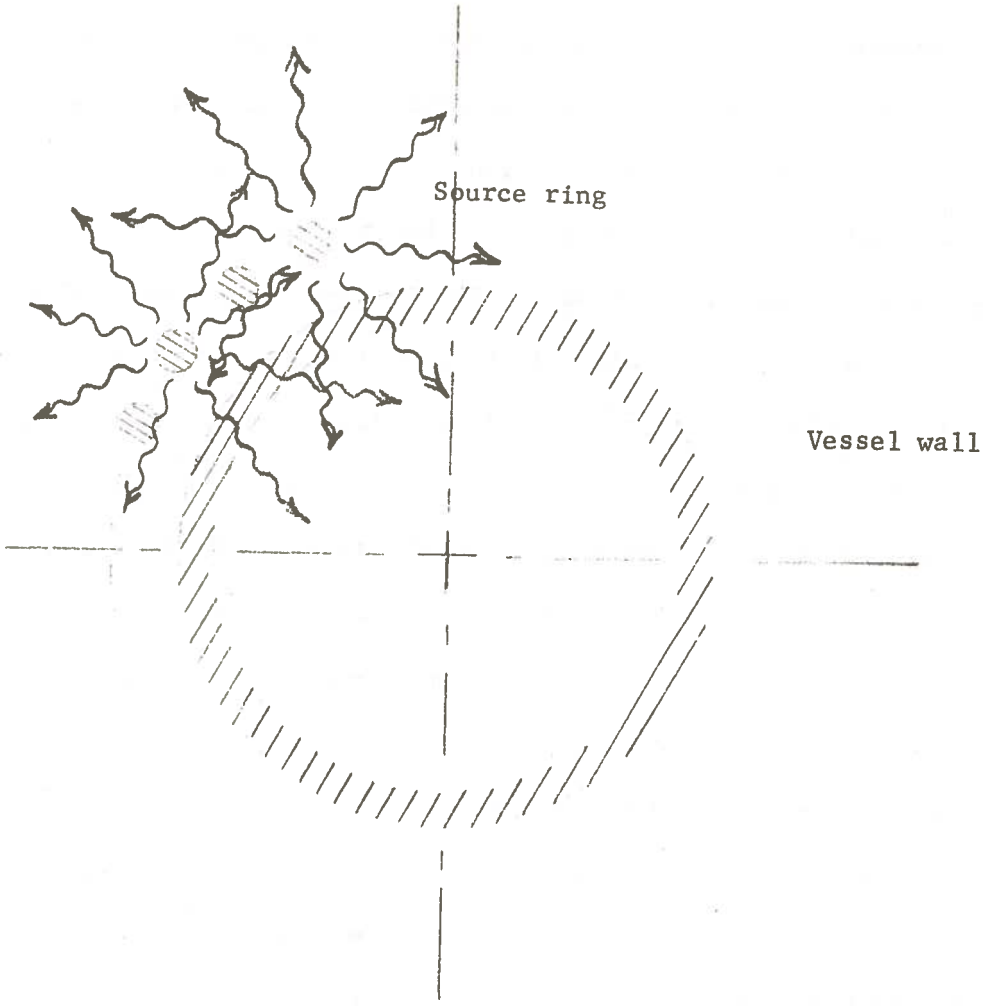

Figure 7: Plane View of a Typical Cylindrical Irradiator Arrangement.

For a practical irradiator there will be biological shielding present. Consequently, a degraded scattering-energy spectrum will be superimposed on the incident primary spectrum. The presence of the scattered spectrum has been neglected in the model, and the incident radiation has been assumed to be monoenergetic. Further, the available sources have been assumed to be at sufficently low energy that pair production is negligible, and the model has included only photoelectric and Compton-scatter interactions. The electron-conversion plates, or walls, have been assumed to be sufficiently thin that multiple interactions within the wall material can be neglected. It is also assumed that thin walls imply negligible degradation of the incident gamma spectrum, so that direct gas-phase gamma interactions are characteristic of the uncollided radiation.

Although a variety of reactive gas mixture could be treated, air has been assumed for the gas-phase. This choice is based upon the quality of information available on the mean excitation energy and energy per ion pair values for air. Standard temperature and pressure have been assumed.

Ion-pair density has been assumed as an appropriate output parameter because of the calculation method and ease with which it can be converted to radiolytic yield.

Wall materials have been assumed to be pure elements to avoid the necessity of calculating effective atomic numbers. Aluminum has been assumed as a typical wall material for initial and detailed calculation.

Basic Approach

Assume the secondary electrons to be generated uniformly by gamma interaction with the wall material of a reaction vessel. These electrons, while traveling in the wall will lose their energy mostly by inelastic collisions with atomic electrons. The nature of the electron absorption curve depends upon the energy spectrum generated in the wall. In a case where only photoelectric interaction occurs the secondary electrons will have the same kinetic energy. The absorption in this case will be similar to that of a monoenergetic electron source which exhibit linear absorption. In a case where only Compton electrons are generated, the polyenergetic spectrum approximates that of a pure beta emitter, for which the absorption curve is approximately exponential. The optimum wall thickness has to be calculated from a spectrum which is a mixture of these two extremes.

The secondary electrons while traveling from the orgin of their production will lose some energy in the wall. The optimum wall separation will depend upon the residual energy of the secondary electrons escaping into the gas phase.

Theoretical calculation for residual kinetic energy of secondary electrons is almost impossible without the help of the computer. However, no standard computer program has been developed to calculate the kinetic energy of the secondary electrons during subsequent slowing down. Furthermore, the cross section for production of low energy secondaries are not well known. For example existing Monte Carlo codes take into consideration only those electrons for

which Bremsstrahlung interaction takes place, other electrons with lower kinetic energy are assumed to disspitate their energy on the spot where they originate.[21]

For these reasons, an approximate method of evaluating electron attenuation has been adopted.

Cavity ionization chambers are used for the measurements of absorbed dose in a medium. A gas-filled space in a solid medium, generally referred to as a cavity, is exposed to radiation and the absorbed dose in the walls of the chamber is determined from the measured ionization in the cavity. This method of dosimetery utilizes the Bragg-Gray theory of the cavity ionization chamber.[22] If S is the ratio of the electron stopping powers of the wall material and gas, then according to the Bragg-Gray theory the energy lost by the secondary electrons per unit volumes in the gas is 1/S times the energy lost by the electrons per unit volume in the wall material. If the distance between two walls is equal to S times the thickness of the wall then according to this theory the total energy absorbed by the wall material is equal to the energy absorbed by the gas.

It is necessary to take into account the effect of the electrons generated by the interaction of the secondary electrons with the atomic electrons of the interacting materfal. The Spencer-Attix theory for the cavity ionization chamber takes into account the effect of these electrons. The stopping power ratio calculated by the Spencer-Attix theory can be applied accurately for the model here. First, we will calculate the ionization produced in the gas for a simple model consisting of two parallel plates and

monodirectional monoenergetic beams of gamma radiation passing through these plates, as shown in Figure 8.

Ionization will be calculated for different wall separations to select optimum wall separation for a previously selected wall thickness.

Two Parallel Plate Geometry with Monodirectional Irradiation

Consider a monodirectional and monoenergetic incident beam of gamma radiation passing through two parallel pates as shown in Figure 8. Assume the thickness of the plates is x_p and the distance between these plates is x_c. Let E_γ be the energy of the incident gamma radiation.

Average Electron Energy

Let τ be the linear attenuation coefficients for photo-electric interaction and σ be the kinetic energy of the produced by photoelectric interaction as given by Equation (1)

$$(T)\text{photo} = E_\gamma - B_e$$

where [23]

$$B_e = \frac{1}{2} m_o c^2 \left(Z_{eff}/137\right)^2 \qquad (25)$$

where

Z_{eff} = effective nucleus charge = Z-0.3

$m_o c^2$ = rest energy of electron = 0.511 Mev.

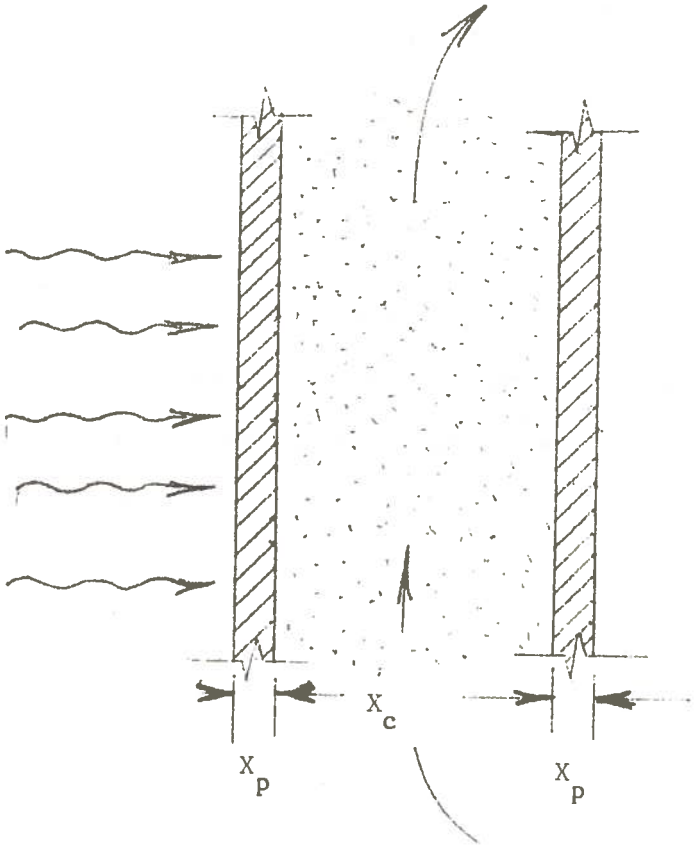

Figure 8: Geometric Arrangement Assumed for the Calculation Model.

In the case of Pb, B_e = 0.0904 Mev and in case of Al, B_e = 0.00219 Mev.

Let σ be the linear attenuation coefficient for Compton interaction. If the average energy per Compton electron is represented by $(\bar{T})_{Compton}$ then $(\bar{T})_{Compton}$ is given by Equation (13) as follows:

$$(\bar{T})_{Compton} = E_\gamma \cdot \frac{e\sigma_a}{e\sigma} .$$

and $_e\sigma_a$ and $_e\sigma$ will be calculated by the Klein-Nishina formula (i.e., Equations (8), (9) and (10).)

The average energy of electrons generated by photoelectric and Compton interactions is calculated as follows:

$$(T)_{av} = (T)_{photo} \times \frac{\tau}{\mu} + (T)_{Compton} \times \frac{\sigma}{\mu} \qquad (26)$$

where

$$\mu = \tau + \sigma$$

The range of electrons of kinetic energy $(T)_{av}$ will be [24]

$$R = 412\left[(T)_{av}\right]^{\eta}$$

where

$$\eta = 1.265 - 0.095\mu \ln\left[(T)_{av}\right]$$

The dimension of R is mg/cm^2. When R is divided by the density of the material, the range of electrons of average kinetic energy in units of centimeter can be calculated.

As a first approximation, the electron generation within the wall material may be assumed uniform. If most of the electrons have the same kinetic energy (as in the case of photoelectrons) and the

thickness of the wall is just equal to the range of these elctrons in the wall material, then referring to Figure 9 the electrons generated in the layer close to the face A will just be able to travel to the opposite face B, but other electrons may penetrate it. Referring to the number versus distance curve for monoenergetic electrons (Figure 10), the practical range, R_p, is found by extrapolating the more or less linear portion of the curve to intersect the background; the maximum range R_o is the point where the curve merges with the background. Both ranges are characteristic of original electron energy. It is clear that if the absorber is equal to one half the maximum electron range in thickness, that fifty percent of the electrons generated in the first thickness dx, of the absorber (entrance side for gammas) will be able to escape into the gas. These electrons will have sufficient residual energy to cause ionization, and therefore be considered "useful" electrons. Greater than fifty percent of the electrons will be able to escape from the second, third, and subsequent layers. Hence, the total number of escaping electrons will be significantly greater than fifty percent of the those generated in the wall. Now, if the wall is greater in thickness than half the maximum range, relatively few of the electrons generated in the first layers would escape, and would be so degraded in energy that they would contribute little to ionization in the gas.

The same argument can be applied to any given fraction of the range. Maximum electron escape would be observed for an infinitely thin wall, whereas maximum electron production would be observed for a wall with a thickness just greater than the electron range. There

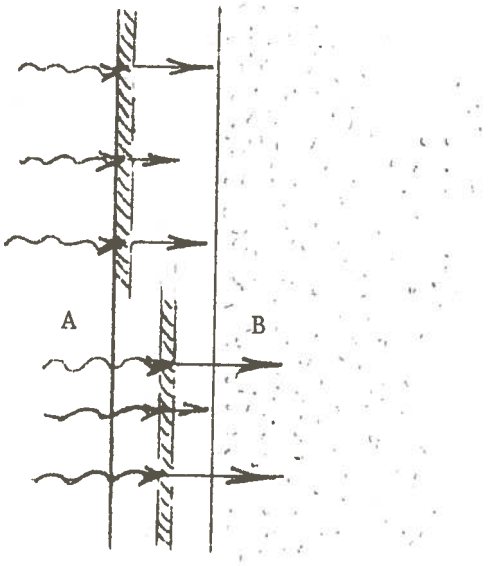

Figure 9: Secondary Electron Absorption and Escape.

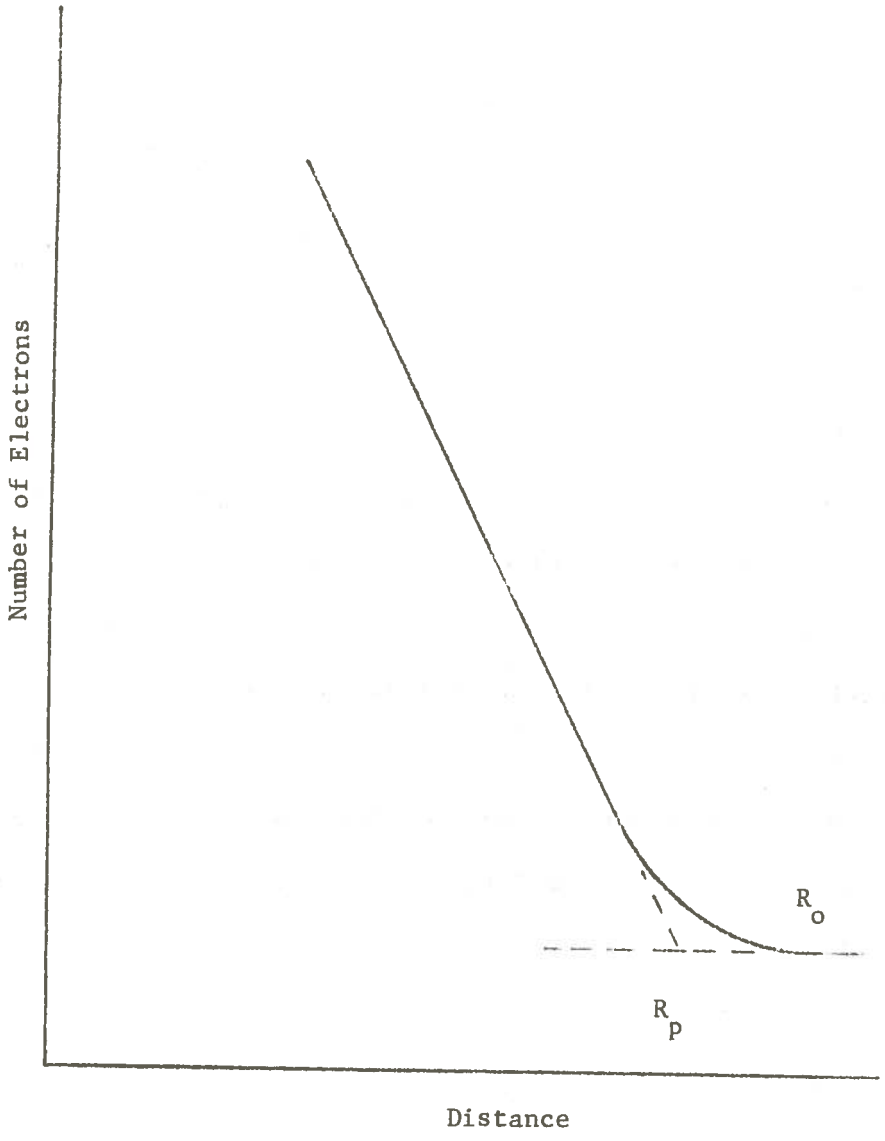

Figure 10: Definitions of Extrapolated (R_p) and Maximum (R_o) Ranges for Monoenergetic Electrons.

appears, therefore, to be no straightforward mathematical function with a unique maximum from which to establish an optimum wall thickness. Rather, an arbitrary choice must be made, in which the residual electron energy is balanced against number yield of electrons.

The wall thickness that has been chosen for this model is given by

$$x_p = \frac{1}{2} R$$

in which R is the range of the average energy electrons generated in the wall. This assumption will assure a reasonable yield of electrons with sufficient residual energy to assure reasonable ion-pair density in the gas. A wall of this thickness will be significantly less than the mean free path of even scattered gamma radiation, which restricts consideration to first-collision interaction only and therefore simplifies calculational requirements for the model.

But monoenergetic electron generation is true in a case where only the photoelectric process occurs. Moreover, electrons are not characterized by linear paths and discrete ranges. Particularly at low energies, an electron path is tortuous as the result of multiple-scattering encounters with nuclei and electrons. The energy distribution of Compton electrons is shown in Figure 6 from which it is clear that the assumption of monoenergetic electrons is an oversimplification. Compton electrons could be compared with the continuous energy distribution of a pure beta emitter. The linear absorption for monoenergetic electrons differs sharpley from

that observed for the continuous energy distribution of a pure beta emitter. Figure 11 shows an approximately linear curve for 1 Mev electrons, between ionization and absorber thickness. Figure 12 shows counts per minute vs. absorber thickness for a pure beta emitter (of continuous energy spectrum) which is approximately an exponential curve.

The rate of electron escape from the wall exhibits an asymptotic approach to a constant value as the thickness of the wall is increased. Figure 13 shows the asymptotic thickness for linear absorption (monoenergetic spectrum) and exponential absorption (polyenergetic distribution). If the wall thickness is greater than the infinite absorber thickness for the linear-absorption assumption, maximum electron yield is assured.

Most of the electrons emerging from the wall will be the electrons generated in layers very close to the face B. Gray has shown that although range of the most energetic electrons generated by radium gamma rays is 7-6 mm in graphite, about two-thirds of the electrons emerging from the wall were generated within a 0.2 mm layer close to the wall.[25] Although the optimum thickness claculated by assuming linear energy distribution is greater than that in the case of exponential energy distribution there will be no significant reduction in the number of electrons emerging from the wall. So in a case where Compton interaction is predominant, wall thickness should be calculated from the range of the most energetic electrons, and assuming electrons lose their energy based on the linear-energy-distribution model.

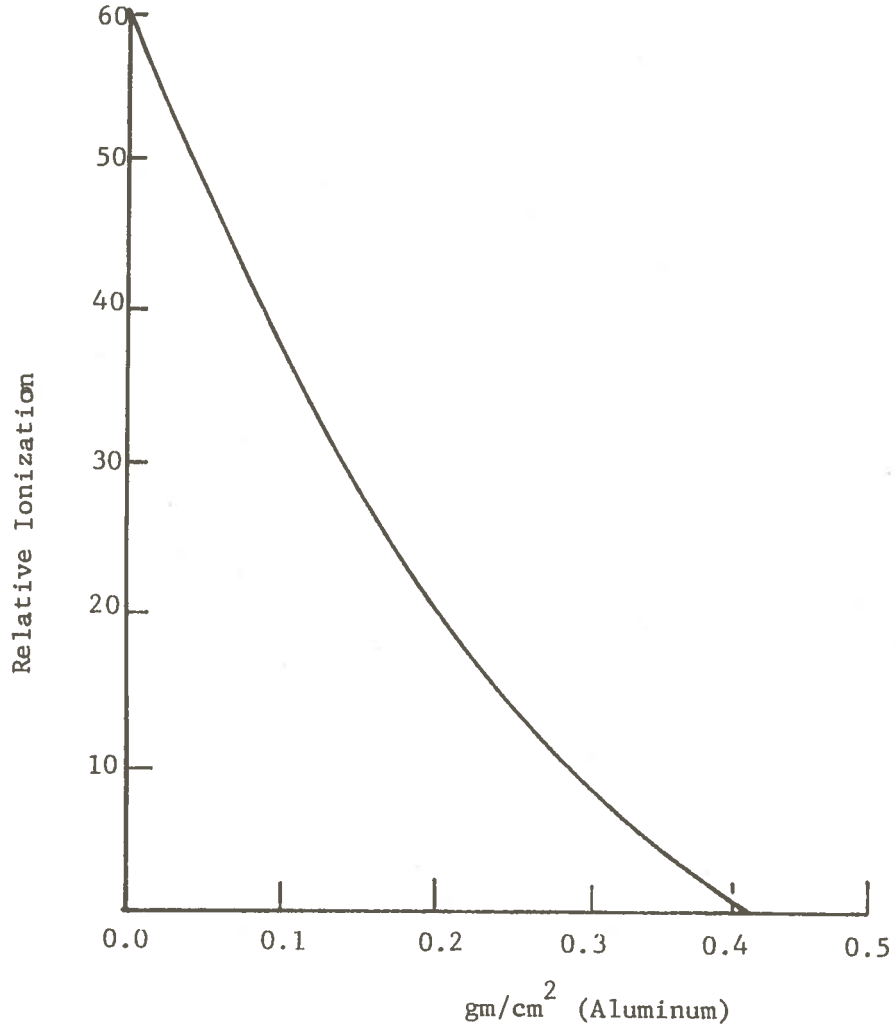

Figure 11: Absorption of 1 Mev Electrons (Linear Energy Distribution).[36]

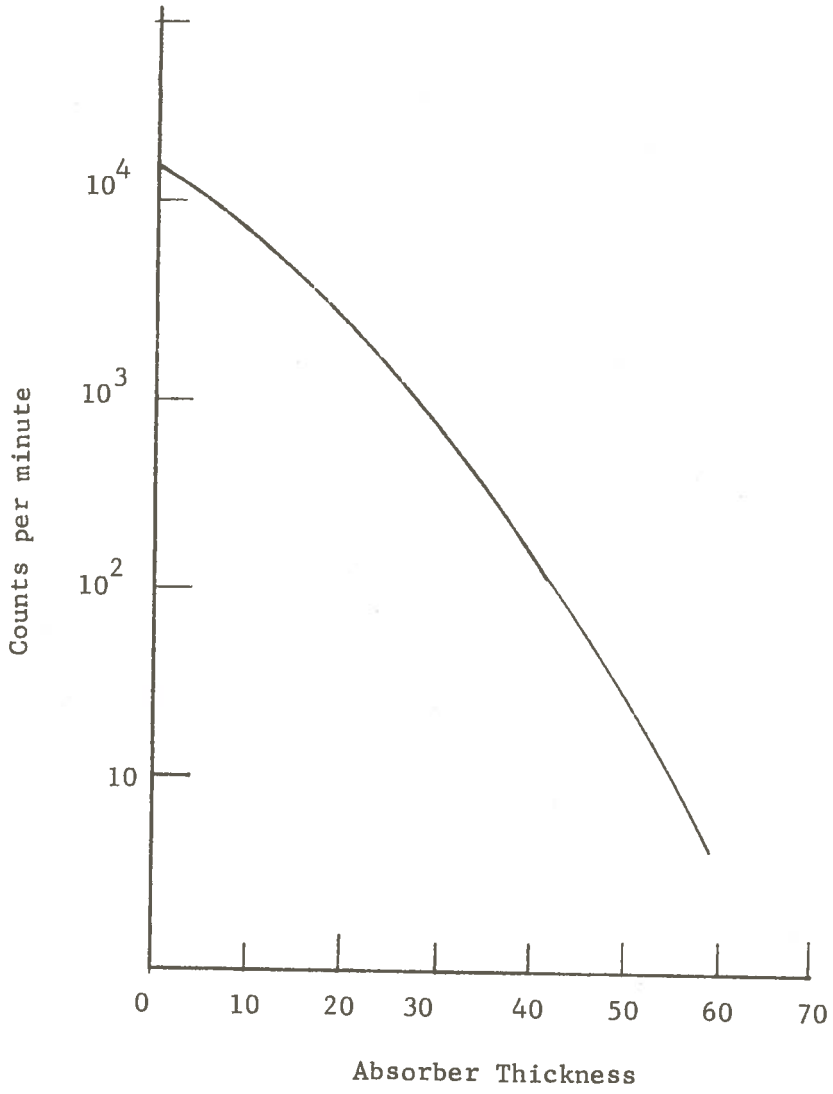

Figure 12: Continuous Energy Distribution of a Pure Beta Emitter Ca-45 with E_{max} = 0.45 Mev.[36]

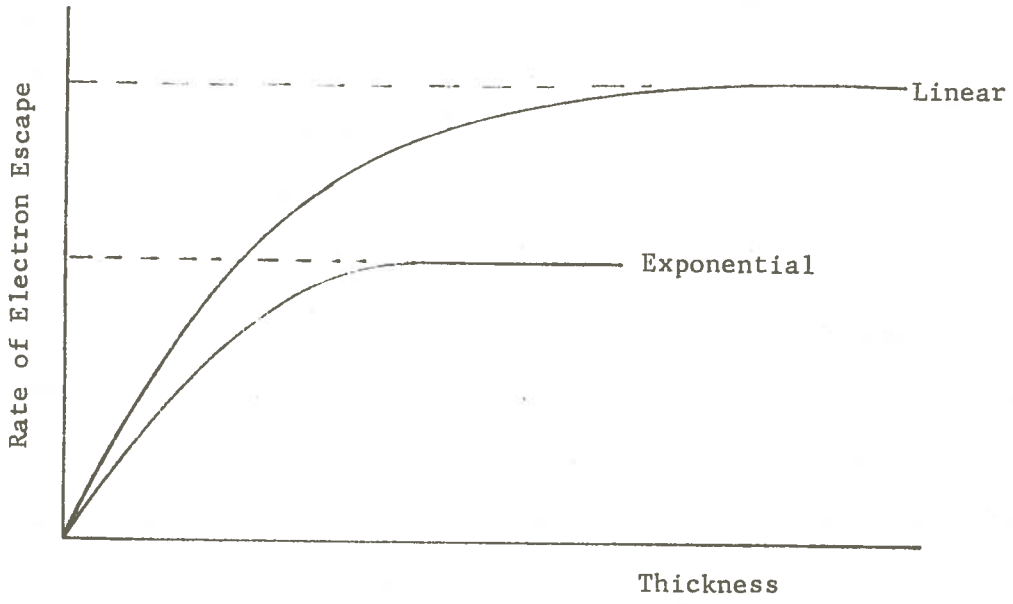

Figure 13: Asymptotic Thickness for Linear Absorption and Exponential Absorption.

Wall Separation

The secondary electrons produced in the wall material, which traveling from the origin of their production to the surface, will lose some energy in the wall. If we could calculate the most probable energy of electrons at the surface of the wall, we could calculate an optimum wall separation, which will be equal to the mean range in gas of these electrons. The range of electrons in the gas depends on the density of the gas and hence on the pressure and the temperature of the gas. The pressure and temperature conditions of gas will depend upon the optimum requirements of the chemical reaction in the gas phase.

For example, Check and Linnenbum have investigated the formation of ammonia in mixtures of nitrogen and hydrogen, exposed to Co-60 gamma radiation, at different gas pressures. The ammonia concentration depends on the total pressure of nitrogen and hydrogen. Thus they have suggested the optimum pressure for hydrogen at 14 atmospheres, and the otpimum pressure of nitrogen as 34 atmospheres.[26]

Consider an electron produced in the layer very near to the face B in Figure 10. It will emerge from the wall with maximum energy. The maximum range of this electron in a gas at fixed pressure will be of many orders greater than the range in a solid material. For example the range of a photoelectron, produced by 1.25 Mev Gamma (Co-60) interaction with aluminum, will be approximately 326 centimeters in air at standard temperature and pressure.[27] To ensure all the electrons emerging out from the wall lose all their energy in the gas itself we would design a wall separation of the order of 326 centimeters. But in this case energy absorbed per

unit volume of the gas (i.e., the energy density) will be minimal. Moreover, wall separation of the order of several hundred centimeters is not suitable for practical purposes. The optimum wall separation will depend upon the nature of the curve for energy density versus total energy dissipated by direct gamma interaction in the gas plus the energy of secondary wall electrons traversing the gas.

A specific example of the effect of wall separation for a condensed system is to be found in the case of Fricke chemical dosimetry. J. Weiss[4] measured the concentration of Fe^{3+} ions in solution, when exposed to Co-60 gamma radiation, for different diameters of a reaction vessel. The results of this investigation is shown in Figure 14. It is clear that in the case of small-diameter reaction vessels there is an increase in reaction rate. With a large enough diameter vessel, the secondary wall electrons will still be present, but their relative contribution to absorbed dose will be negligible. The liquid near the walls receives more secondary electrons than the liquid away from the wall. R. Puig and Sutton[28] have developed empirically the thickness of the influencial zone (where reaction rate is dependent on wall separation) for the Fricke dosimeter. Their empirical approach is based on experimental results obtained for various diameters of a cylinderical reaction vessel.

One would expect similar behavior in the case of irradiation of gases. Various ionization chambers (cavity-chamber) have been used for measurement in radiation dosimetery. A cavity chamber has a gas-filled space in a solid medium. Whyte[29] has done experimental work to study the effect of wall separation on the ionization

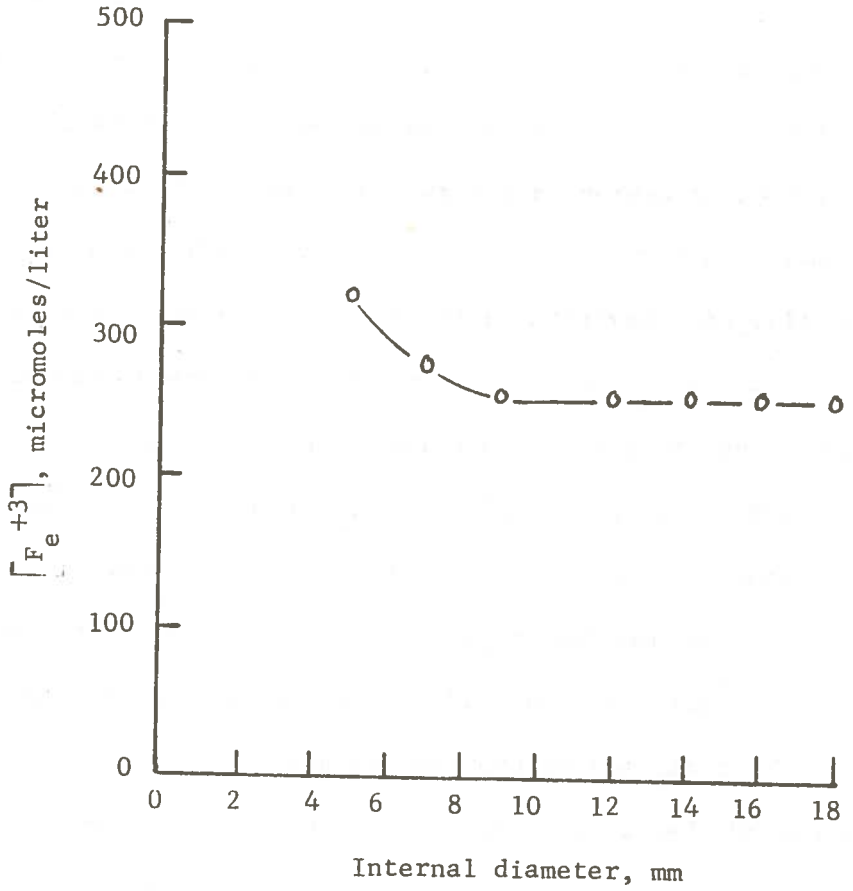

Figure 14: Effect of Vessel Diameter on Yield for Fricke Chemical Dosimetry.[4]

produced in the cavity of the different wall materials. Bragg and Gray[22] were the first to develop basic formulas relating the ionization in a cavity chamber to the energy absorbed in the chamber wall material. Ionization in the gas of a cavity can be calculated from the ratio of the mass stopping powers of the wall material and the gas in the cavity.

An experimental plot of ionization produced in the cavity is shown in Figure 15 for different wall materials. As the distance between the walls decreases the ionization increases, so that in the hypothetical case of a very thin layer of gas enclosed between two solid plates maximum ionization would be observed. As wall separation increases, there is a decrease in the ionization produced per unit volume in the gas; after a certain wall separation is reached, however, specific ionization becomes almost constant. The wall separation at which specific ionization becomes just constant will be the best distance between two walls for maximum energy utilization. In order to calculate this distance between two walls, it is important to calculate the ratio of energy absorbed by the gas to the energy absorbed by the wall material. This ratio is called the stopping power ratio and is denoted S_v or S_m, when speaking of energy absorbed per cubic centimeter or per gram, respectively.

Since the thickness of the wall material has been established from previous considerations, we can calculate the energy absorbed per gram or per cubic centimeter by the wall material, and hence the energy absorbed per gram or per cubic centimeter by the gas. Knowing the specific ionization (in the gas) at the average residual

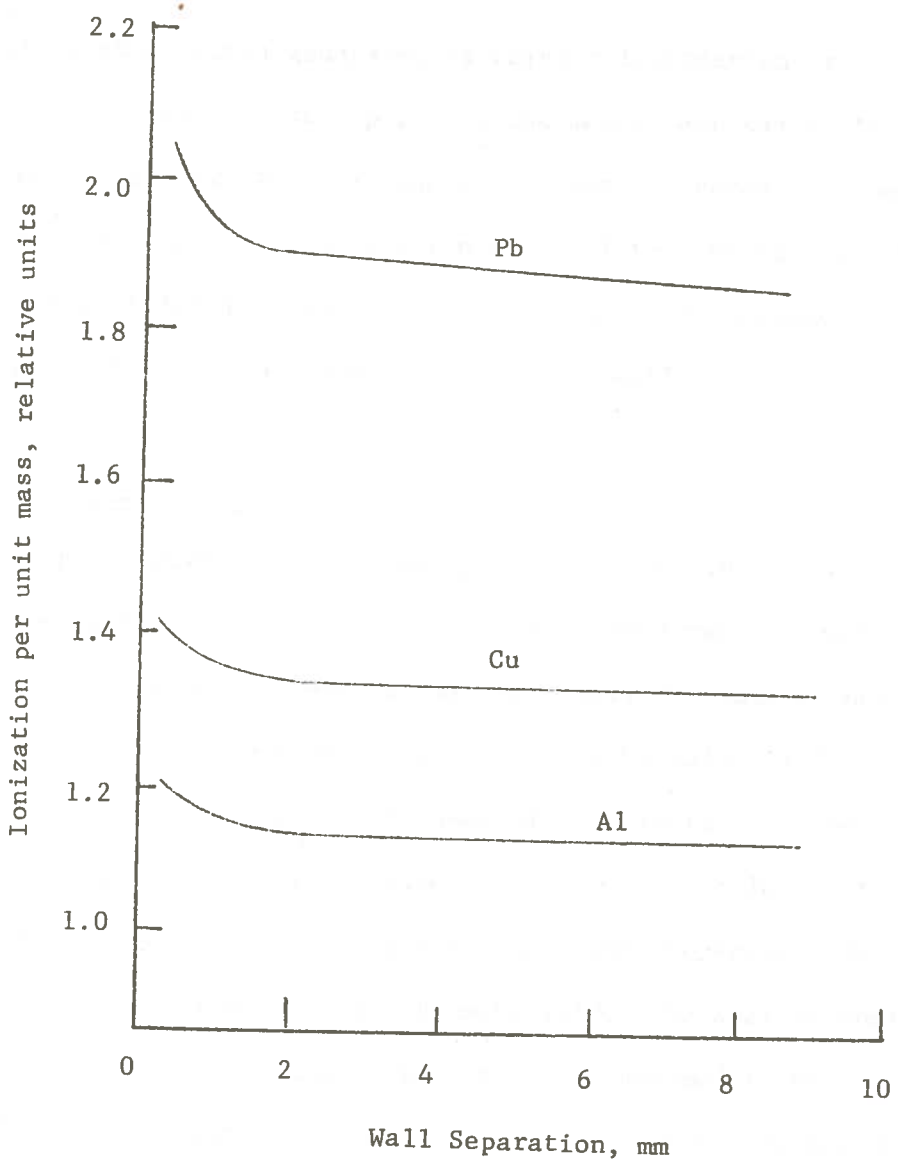

Figure 15: Variation of Ionization with Wall Separation. [29]

electron energy on reaching the surface of the wall, the wall separation can be calculated.

Consider an electron generated by Compton interaction or photoelectric interaction at a point in the medium and calculate its residual energy on reaching the boundary. Energy absorbed by the gas can be calculated by intergaration over all the initial electron energies out to a distance from the wall to the maximum range of the most energetic electrons emerging from the wall.

Stopping Power Ratio

The stopping power ratio is needed in the determination of the exposure does from ionization measurements in a cavity chamber. This has led to the development of various cavity ionization theories. Gray[22] derived a "principle of equivalence", to be valid if the cavity was small compared with the range of the electrons. The principle of equivalence may be stated as: "The energy lost per unit volume by electrons in the cavity is S_v time the energy lost by γ rays per unit volume of the wall material". The average energy disipated in the gas per ion pair formed, W, is assumed to be independent of the electron energy, so that the energy absorbed per unit volume of gas is $J_v W$, where J_v is the ionization per unit volume of gas. If E_v is the energy absorbed per unit volume of the wall material, then

$$E_v = S.W.\ J_v. \qquad (28)$$

This is the Bragg-Gray relation. Laurence[30] provided formulation and data to take into account the face that the stopping power ratio for electrons is not independent of their energy.

Laurence's Derivation[30]

For calculations, Laurence considered the electron flux coming from all the production sites out to the maximum electron range from the cavity, considering also the energy lost by each electron before arriving at the cavity. Let $F(r_w-x)$ be the number of ion pairs produced per centimeter of path in a cavity for an electron that originated at a distance r_w via the wall material, and G(T) be the number of the ion pairs per centimeter produced in a cavity by an electron that enters the cavity with energy T. Then,

$$F(r_w-x)\ dx = G(T)\left(\frac{dT}{dx}\right)_w^{-1} dT \tag{29}$$

where $-(dT/dx)_w$ is the linear stopping power if the energy of an electron changes in average of dT in a distance dx along its path. If $(d\mu/dT_o)_w$ is the rate of production in the wall material per cubic centimeter per gamma ray per square centimeter of electrons having initial energies between T_o and $T_o + dT_o$, then the total ionization in the wall material is given by

$$J = \int_o^{T_{max}} \left(\frac{d\mu}{dT_o}\right)_w \int_o^{T_o} \frac{G(T)}{\left(\frac{dT}{dx}\right)_w}\ dT\ dT_o \tag{30}$$

Electronic equilibrium will exist in the wall material (under uniform gamma radiation), if electrons of initial energy T_o Mev are assumed to be generated at a uniform rate per gram per second everywhere in the wall material. The solid is everywhere traversed by an equilibrium electron flux $I_z(T_o,T)$ electrons per cm^2-sec-Mev, the spectrum of which is characteristic of the atomic number Z of the material. Let each electron reaching to the cavity be considered as losing energy continuously (in infinitesimal steps) at a rate ${}_mS_g(T)$ Mev-cm^2/gm. Thus the energy dissipated per gram of the gas dividied by that per gram of wall material is given by the ratio

$$f_z(T_o) = \frac{1}{T_o}\int_o^{T_o} I_z(T_o,T)\ {}_mS_g(T)\ dT \tag{31}$$

If only continuous energy losses are allowed in the wall material also we can write

$$I_z(T_o,T) = \frac{1}{{}_mS_g(T)} \tag{32}$$

then

$$f_z(T_o) = \frac{1}{T_o}\int_o^{T_o} \frac{{}_mS_g(T)}{{}_mS_w(T)}\ dT \tag{33}$$

Equation (33) is useful when only photoelecgric interaction is considered. When there is a spectrum of initial electrons energies $d\mu/dT_o$ (as in the case of Compton interaction), then

$$\bar{f}_Z(T_o) = \frac{\int_o^{T_{max}} \frac{d\mu}{dT_o} \int_o^{T_o} \frac{m^S g(T)}{m^S w(T)} \, dT \, dT_o}{\int_o^{T_{max}} \frac{d\mu}{dT_o} \, T_o \, dT_o} \tag{34}$$

The Laurence treatment has presented a more accurate method than Bragg-Gray's for averaging the stopping power ratio over a spectrum of electrons crossing the cavity. However, the two treatments do not differ basically in approach because both assume a continuous-energy-loss model for electrons. The Laurence theory does not take into account the fact that many of the primary electron collisions produce fast secondary electrons that can travel an appreciable distance in the wall material, and some of these secondary electrons might escape into the cavity. Spencer and Attix have taken into consideration the effect of secondary electrons in their theory which provides more accurate results.

Spencer-Attix Theory[31]

Allowing for the production of fast secondaries requires a basic change in approach to the problem. Such secondaries are produced in the cavity, carrying energy out, and are also produced in the wall material, therefore modifying the spectrum of the electron flux traversing the cavity. A rigorous calculation would involve the complete analysis of the energy disspitated in the cavity including:

a. Energy spent by electrons entering the cavity with insufficient range of to span it.

b. Energy spent by cavity-traversing electrons via production of secondaries incapable of reaching the cavity wall.

c. Energy spent by fast secondaries originating in the cavity with sufficient energy to escape.

d. Energy spent by primary electrons generated by direct gamma ray interaction within the cavity.

The Spencer-Attix theory neglects nuclear scattering as well as primary gamma ray interaction with the gas.

Let Δ be the energy needed by an electron to be able to just cross the wall separation before stopping. It is assumed that all secondaries originating with energy less than Δ are called "slow" and are assumed to dissipate their energy on the spot where they originate or become "slow". All electrons with starting energies greater than Δ carry their energy elsewhere and can thus be regarded as part of the fast electron flux; Δ has to be very much less than T_o ($\Delta = 0.1T_o$ at most) because of assumption 'd' mentioned above. Based on this approach we can write

$$f_Z(T_o,\Delta) = \frac{1}{T_o}\int_{\Delta}^{T_o} I_z(T_o,T)\ S_g(T,\Delta)dT \qquad (35)$$

where T_o in the energy of electrons generated by a uniform gamma ray field of energy E_γ, and $I_z(T_o,T)$ is the fast flux ($T > \Delta$) of primary plus secondary electrons traversing the cavity.

Spencer and Fano[32] express $I_z(T_o,T)$ by

$$I_z(T_o,T) = R_z(T_o,T) \times \left(\frac{dT}{dz}\right)^{-1} \tag{36}$$

where dT/dz = stopping power and $(dT/dz)^{-1}$ is the primary electron spectrum

$$Rz(T_o,T) = \frac{\text{total electron flux (primary + secondary)}}{\text{primary electron flux}}$$

This ratio is energy dependent.

$S_g(T,\Delta)$ = energy transferred to electrons not achieving kinetic energy above Δ per unit path length by an electron of kinetic energy = T.

Theoretical Values of Stopping Power Ratio[33]

The mass stopping power of electrons due to ionization and excitation of atomic electrons in the stopping medium is given by

$$S_m = \frac{2\pi e^4 N Z}{Am_o V^2}\left[\ell n \frac{m_o V^2 E}{4(1-\beta^2)I^2} + 1-\beta^2 + \left(\frac{E}{E + m_o c^2}\right)^2\left(\frac{1}{\gamma} + \ell n^2\right) - \delta\right] \tag{37}$$

It is a somewhat improved form of Equation (21) (all the symbols are same as of Equation (21)). Using the above equation we can rewrite Equation (31) as follows:

$$f_Z(T_o) = \frac{(Z/A)g}{(Z/A)z}\left[1 + \frac{1}{T_o}\int_o^{T_o} \frac{\ell n \frac{I_z}{I_d} + \frac{d_z}{2}\, dT}{e^{B_z}}\right] \tag{38}$$

e^{B_z} is the stopping number per electron and is defined as

$$e^{B} = \frac{Am_o c^2}{4\pi \rho NZe^4 z^2} \left(-\frac{dT}{dx}\right) \tag{39}$$

Z = atomic number

A = atomic weight

e = the charge on the electron

m_o = rest mass of the electron

ρ = density

Z = number of electronic charges

It is convenient to introduce two functions $b_z(T_o)$ and $d_z(T_o)$ defined so that[35]

$$f_Z(T_o) = \frac{(Z/A)_g}{(Z/A)_z} \left[1 + b_z(T_o) \ln \frac{I_z}{I_o} + d_z(T_o)\right] \tag{40}$$

Both functions have been calculated for various energies and materials. Values for b_z and d_z are presented in Tables B-1 and B-2 of Appendix B. Up to a lower energy limits (3 Mev)

$$b_z(T_o) = E_i \left[\frac{\ln \sqrt{\frac{e}{2}} \frac{T_o}{I_z}}{\sqrt{\frac{e}{2}} \frac{T_o}{I_z}} \right] \tag{41}$$

In which E_i is the exponential integral function

$$E_i(x) = \int_{-\infty}^{x} \frac{e^{\mu}\, d\mu}{\mu}$$

$$E_i(-x) = \int_x^{\infty} \frac{e^{-\mu}}{\mu} d\mu$$

The function $b_z(T_o)$ depends on I values chosen for calculations: the dependence is logarithmic. The I values based on Bakker and Segre's work have been used to compute b_z.[34]

The term d_z depends quite strongly on the I values chosen for calculation. Fortunately, however, the d_z term is relative small, so there will be negligible error.

Equation (40) is good for an emitter of monoenergetic electron of energy T_o, distributed uniformly through the wall material. For other cases, $f_z(T_o)$ must be averaged over the spectrum of initial energies, such as secondary electrons from Compton scattering. This can be expressed by

$$\tilde{f}_z(T_\gamma) = \frac{(Z/A)_g}{(Z/A)_z} \left[1 + a_z(T_\gamma) \ln \frac{I_2}{I_g} + D_z(T_\gamma)\right] \qquad (42)$$

where a_z and D_z are averages over b_z and d_z respectively. Results for a_z are presented in Table B-3 and for D_z in Table B-4 in Appendix B.

The Spencer-Attix results for $f_z(T_o,\Delta)$ is given by Equation (35). It can be treated in the same way as in Equation (40). The results may be written in a form very much like Equation (40).

$$f_z(T_o,\Delta) = \frac{(Z/A)_g}{(Z/A)_z} \left[1 + C_z(T_o,\Delta) \ln \frac{I_2}{I_g} + d_z(T_o)\right] \qquad (43)$$

The dependence on Δ, the energy of the electron that can just cross the average dimension of the reaction vessel is through the factor $C_z(T_o,\Delta)$ that replaces $b_z(T_o)$. The results of $C_z(T_o,\Delta)$ are given in Table B-5 in Appendix B.

For Compton spectra, averaging is difficult because there is so little data for $f_z(T_o,\Delta)$. However, $f_z(T_o,\Delta)/f_z(T_o)$ is found to be relatively insensitive to energy and is assumed to be constant at the value it has for $\bar{T}$, the average energy of the recoil electron in the starting spectrum. Then the average value is given by

$$\bar{f}_z(T_o,\Delta) = \frac{f_z(\bar{T},\Delta)}{f_z(\bar{T})} \cdot \bar{f}_z(T_\gamma) \tag{44}$$

and $\bar{f}_z(T_\gamma)$ can be obtained from Equation (42).

Relative Importance of the Photoelectric and Compton Processes

The calculation of $f_z(T_o,\Delta)$ is done as follows:

First calculate $f_z(T_o,\Delta)$ for the photoelectric effect only, and calculate $f_z(T_o,\Delta)$ for Compton electrons. Then the resulting $f_z(T_o,\Delta)$ is given by:

$$f_z(T_o,\Delta) = (f_z(T_o,\Delta) \text{ in case of PE}) \left(\frac{\tau}{\mu}\right) + (f_z(T_o,\Delta) \text{ in case of Compton interaction}) \left(\frac{\sigma}{\mu}\right)$$

where

$$\mu = \tau + \sigma$$

Mixed Gamma Energy Source

The function $f_z(T_o,\Delta)$ is calculated for each energy as described above. The average value of $f_z(T_o,\Delta)$ will be the simple arithmetic average of values of $f_z(T_o,\Delta)$ calculated for each energy.

The calculation of $f_z(T_o,\Delta)$ then can be related to the optimum wall separation calculations as follows:

Referring to Equation (28) it is clear that the stopping power ratio, $f_z(T_o,\Delta)$ is directly proportional to the ionization produced per unit mass of the gas. $f_z(T_o,\Delta)$ will be calculated for different wall separations. The optimum wall separation will be that when the ionization produced in the unit mass of the gas does not vary with further increase in the wall separation. Figure 15 shows a curve of ion pair density across the channel width.

Polydirectional Radiation

Let us consider now the case of two parallel plates exposed to beams of gamma radiation from both sides as shown in Figure 16 Ion pair density, corresponding to the secondary electrons produced in the wall, I, across the channel width is shown by curve 1 in Figure 16, while ion pair density, corresponding to the secondary electrons produced in the wall, II, across the channel width is shown by curve 2. Curve 3 in Figure 16 is the linear addition of curves 1 and 2, and thus represents total ion pair density across the channel width. The total ion pair density is quite uniform across the channel width, and the optimum channel width will be the same as calculated previously.

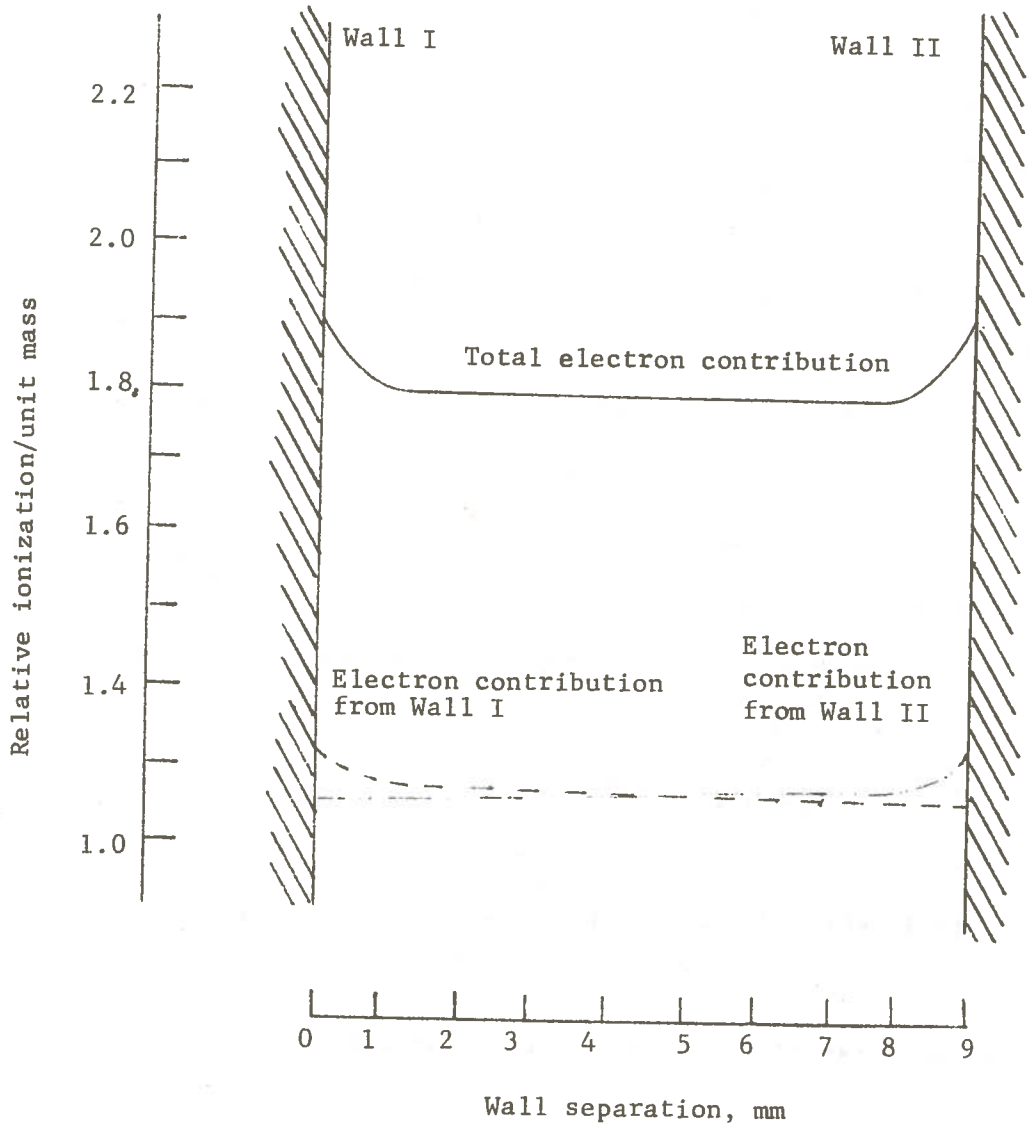

Figure 16: Theoretical Gas-Phase Dose Rate Contribution for Bidirectional Radiation (Results from Chapter IV)

CHAPTER IV

RESULTS AND DISCUSSION

Discussions in the preceding chapters have developed the basis of a model to evaluate the extent to which the radiation dose rate in a gas during gamma irradiation can be augmented by electrons ejected from the surfaces of metal plates included in a reaction chamber. Although in the case of a operational radiolysis chamber the incident radiation will be multidirectional and polyenergetic, and a complex geometry of electron-conversion plates would probably be introduced, the fundamental question of possible dose-rate augmentation can be investigated through a simplified model. This simplified model assumes monoenergetic incident gamma radiation delivered as a collimated beam perpendicular to a single pair of infinite plane parallel plates defining the gas volume. The response parameter chosen to reflect dose-rate augmentation is the number of ion pairs formed per unit volume. Only if the prediction of this idealized model are encouraging would it be worth attempting to extend computations to a more realistic situations amenable to experimental verification.

Calculation Technique

Considering the case of two parallel plates exposed to a mon-directional beam of monoenergetic gamma radiation, it has been established in the previous chapters that the plate thickness can be calculated by assuming a linear energy distribution of the

secondary wall electrons, with the proper thickness being chosen as equal to one half of the maximum range of electrons of average energy. The average electron energy is calculated by Equation (26):

$$(T)_{av} + (T)_{photon} \times \frac{\tau}{\mu} + (\bar{T})_{Compton} \times \frac{\sigma}{\mu}$$

where

$$\mu = \tau + \sigma$$

For the selected wall separation it is required to calculate the stopping power ratios, defined as the ratio of the energy absorbed per unit mass of the gas to the energy absorbed per unit mass of the wall material. Let this ratio be denoted by S. By Equation (28) the energy absorbed per unit mass of gas is:

$$E_M = S.W. J_M$$

where

J_M = ionization per unit mass of the gas

W = the average energy dissipated in the gas per ion pairs formed.

Hence,

$$\therefore J_M = \frac{E_M}{SW_M} \qquad (46)$$

The Spencer-Attix theory, discussed previously in Chapter III, has been assumed for the calculations of stopping-power ratios to include proper energy dependence. Mathematically, the model is designed to calculate S, and hence ionization per unit mass of the gas, for different wall separations. From the curve of ionization

per unit mass of the gas as a function of wall separation, proper wall separation can be chosen. Proper separation is considered to be that distance at which ionization per unit mass of the gas becomes essentially constant.

The Spencer-Attix theory is applicable only for a wall separation which is less than the range of the maximum energy secondary electrons in the gas. Let T_o be the kinetic energy of the maximum energy secondary electron, and let the energy of an electron necessary to just cross a channel to be designated as Δ; then for the application of Spencer-Attix theory,

$\Delta \ll T_o$ ($\Delta < 0.1\ T_o$ at the most). If R is the range in the gas of an electron of the energy Δ, then R is equal to the distance between two walls. Calculations are made for different Δ's, which then will correspond to different wall separations depending upon the range R.

Figure 17 is a flow diagram of the Fortran IV program used for calculations of wall thickness and stopping power ratios at different wall separations. The table functions $d_z(T)$, $b_z(T)$, $D_z(T_\gamma)$, $A_z(T_\gamma)$ and $C_z(T,\Delta)$, as described in Chapter III, are stored as arrays X1,(I,J), X2(I,J), X3(I,J), X4(I,J) and X5(I,J). The input data required for this program is the energy of the gamma source and the literature value of the photoelectric cross section of the wall material. Also required are the values of atomic weight, atomic number, and the values of ionization potentials for the wall material and the gas. The program is divided into two parts to calculate the optimum thickness and the mass stopping power ratio S.

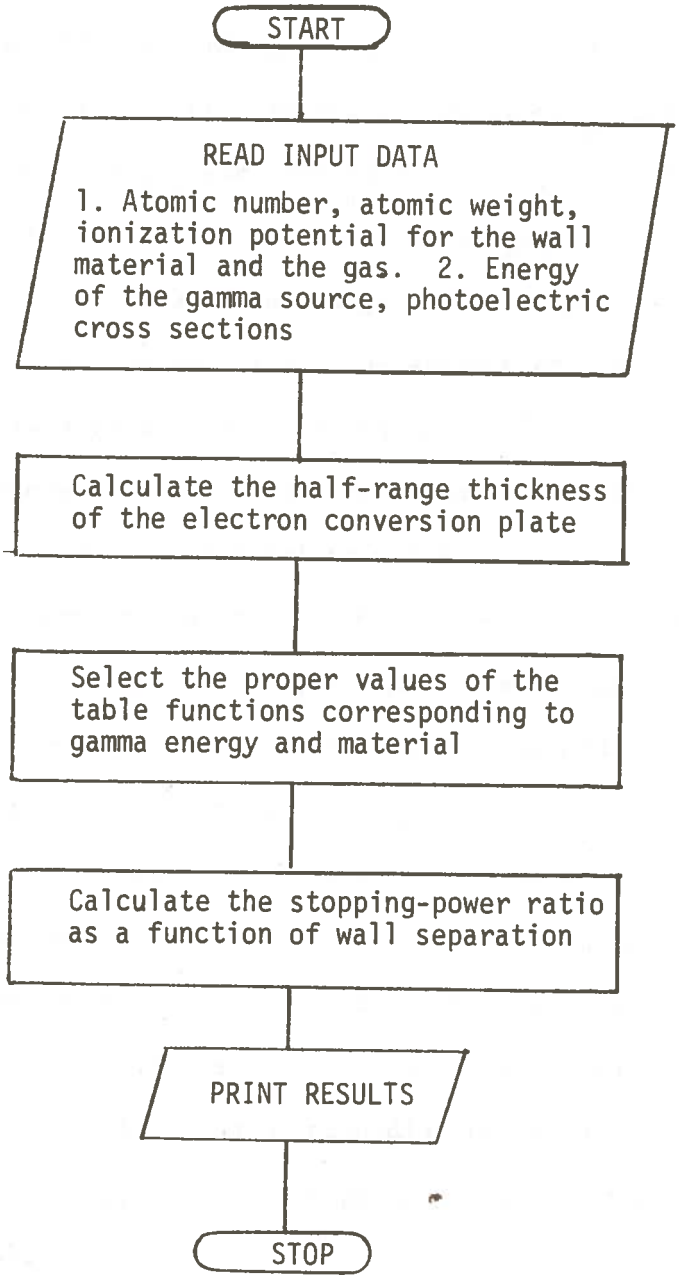

Figure 17: Flow Diagram of the Computer Program.

To obtain electron-plate thickness the program first calculates the average energy of the photoelectrons by using equation (1), with the average value of the binding energy calculated by Equation (25). The total electronic Compton absorption coefficent $_{e}\sigma$ the Compton scattering coefficient $_{e}\sigma_{s}$ are then calculated by using Equations (8) and (9). The Compton absorption coefficients $_{e}\sigma_{a}$ is calculated by Equation (10). Then the average energy of the Compton electrons is calculated by using Equation (13). The average energy of the secondary electrons is calculated by Equation (26). The range of these average energy electrons is then calculated by Equation (24). The thickness of the wall is equal to 0.5 R.

The second part of the program deals with calculations of the stopping power ratio S. First, F_1 is calculated by using Equation (43) for different values of Δ provided in the program and by selecting appropriate value of the functions C_z and d_z according to the average energy of the Compton electrons and Δ value. F_2 is then calculated by using Equation (40). The values of table functions b_z and d_z are selected according to the average energy of the Compton electrons. F_3 is then calculated by using Equation (42) and selecting values of a_z and D_z according to the energy of the gamma source. Finally, the mean stopping power ratios is calculated by Equation (44).

The selection of the table functions is done by comparing respective energy with the first element of each row and selecting that value of the first element which is closest to the energy for which the table function is required. Depending upon the material,

the proper column is selected which gives the value of the table function. The complete computer program is given in the Appendix A.

Results

The mass stopping power ratio S and the wall thicknesses for aluminum and photon energies of 0.66 Mev (Cs-137 gammas) and 1.25 Mev (the average energy of Co-60 gammas) are presented in Tables 1 and 2 as calculated by the computer progran. The wall separation is according to the range of the electrons in air at standard temperature and standard pressure.

Now referring to Equation (46) the ionization per unit volume of the gas is directly proportional to 1/S. For a given wall material and gas, E_M (the energy absorbed per unit mass of the material) and W (the average energy dissipated in the gas per ion pair formed) are constant for a particular energy of the gamma source. Therefore, a plot between 1/S and wall separation essentially respresents a plot of the ionization per unit mass of the gas of a function of wall separation. Figure 18 and Figure 19 respectively show these plots for the two cases mentioned earlier.

It is clear from Figures 18 and 19 that ionization per unit mass of the gas is maximum for a very thin layer of gas next to the wall. Ionization per unit mass of the gas decreases as wall separation is increased. Decrease in specific ionization is rapid until a wall separation of 6 to 7mm is reached while between 7mm to 22mm specific ionization changes slowly and could be assumed constant. To utilize the effect of secondary electrons a wall separation could be chosen as 10mm at the most.

TABLE 1

Calculated Stopping Power Ratios for Various Wall Separations

Cs-137 Source (Aluminum Wall)
Half-range Thickness = 0.13mm

	Wall Separation (mm)	Δ (Kev)	S_m	$\frac{1}{S_m}$
1	0.150	2.56	0.811	1.233
2	0.510	5.12	0.828	1.207
3	1.900	10.24	0.842	1.187
4	6.400	20.48	0.852	1.173
5	22.00	40.96	0.862	1.160
6	73.00	81.82	0.870	1.149

TABLE 2

Calculated Stopping Power Ratios for Various Wall Separations

Co-60 Source (Aluminum Wall)
Half-range Thickness = 0.44mm

	Wall Separation (mm)	Δ (Kev)	S_m	$\frac{1}{S_m}$
1	0.150	2.56	0.812	1.231
2	0.510	5.12	0.829	1.206
3	1.900	10.24	0.842	1.187
4	6.400	20.48	0.852	1.173
5	22.00	40.96	0.861	1.161
6	73.00	81.82	0.868	1.152

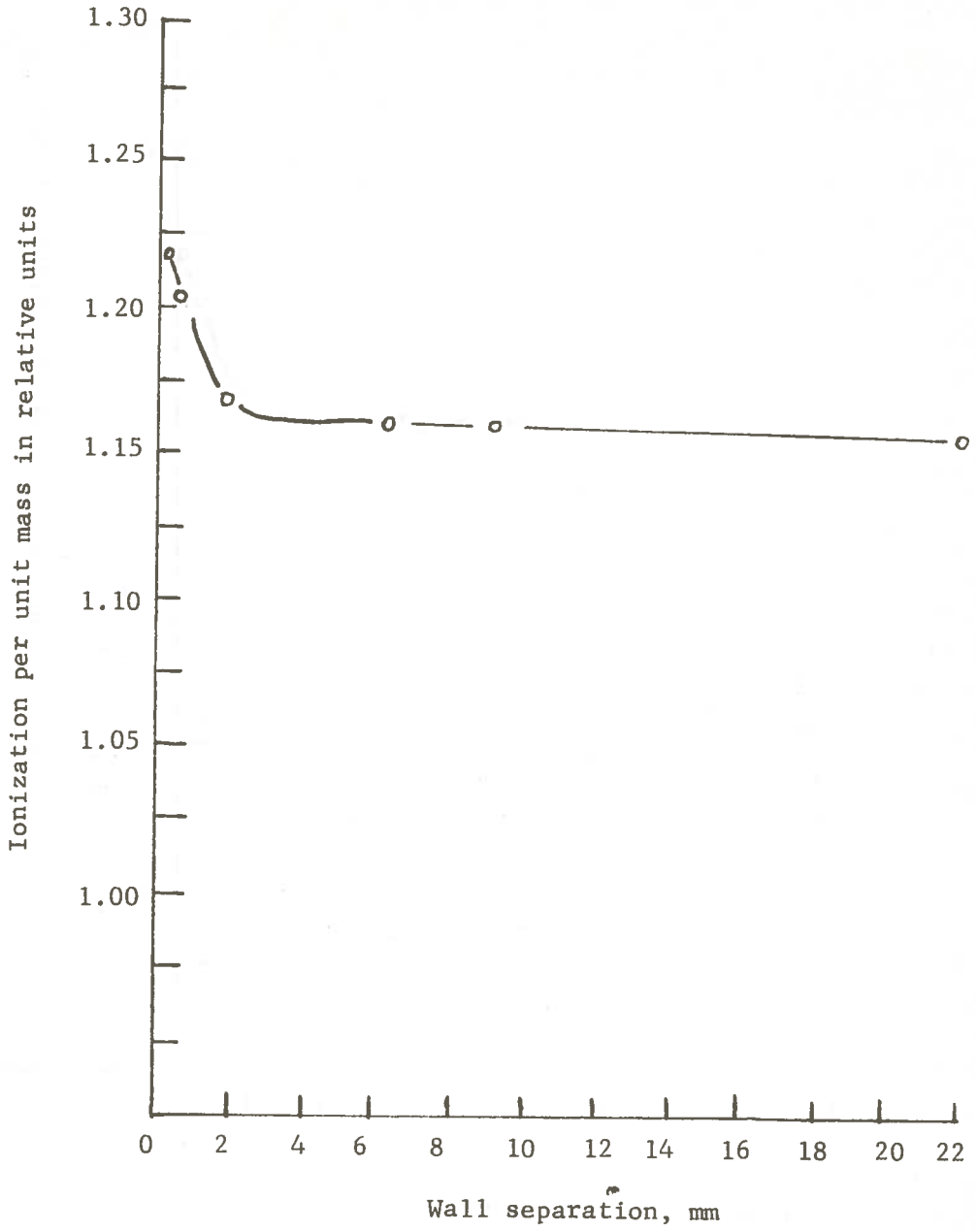

Figure 18: Calculated Values of Ionization Per Unit Mass of the Gas for Aluminum Conversion Plates and Cs-137 as a Function of Wall Separation.

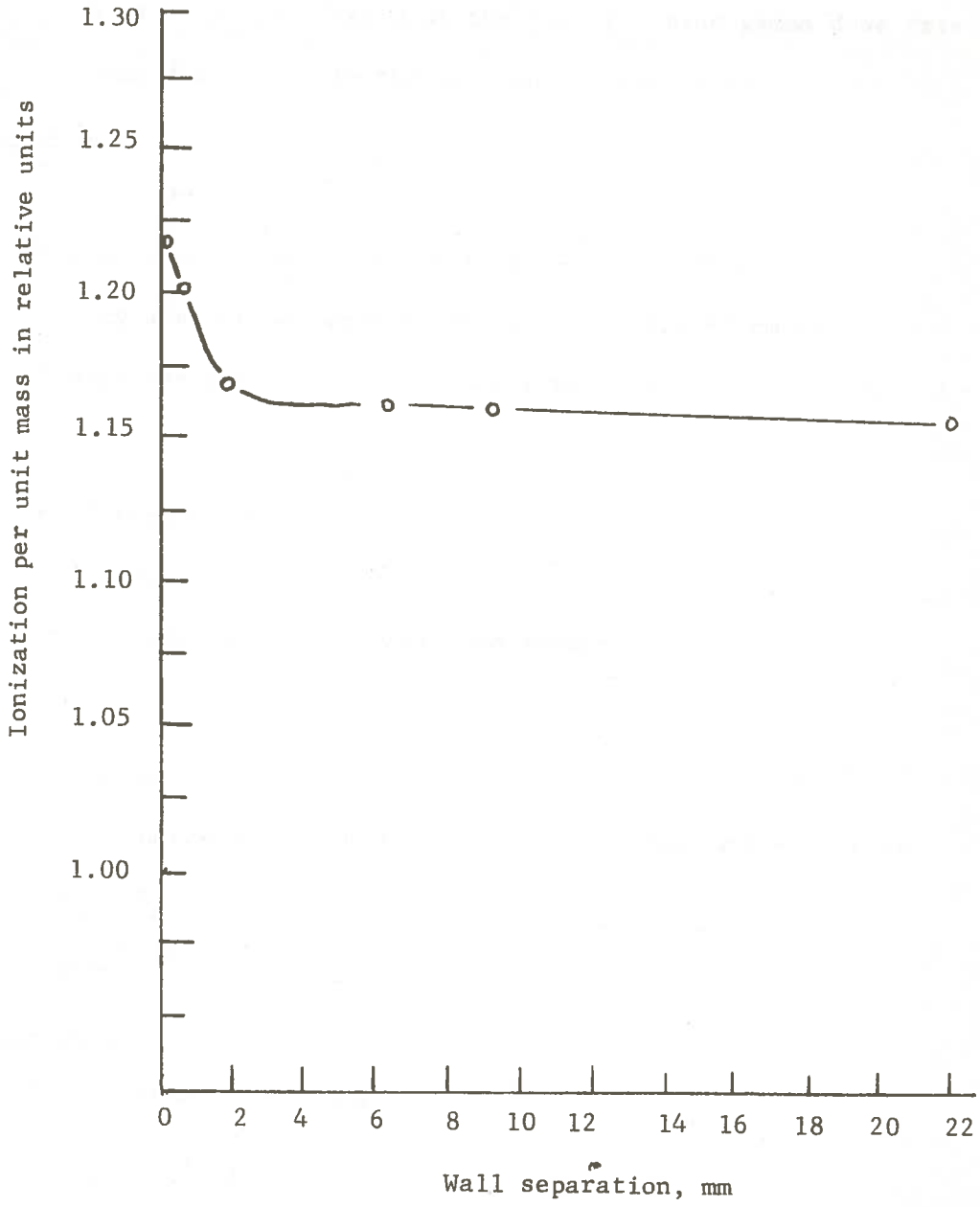

Figure 19: Calculated Values of Ionization Unit Mass of the Gas for Aluminum Conversion Plates and Co-60 as a Function of Wall Separation.

At the chosen wall separation of 10mm, and an aluminum wall thickness of 0.5 R, the ratio of the electron plus gamma dose rate to the gamma dose alone in the gas can be calculated.

Cesium 137:

1/S at 10mm = 1.169

Energy absorption coefficient for Al = 0.0282 cm^2/g

Energy absorption coefficient for air = 0.0292 cm^2/g

Energy absorbed in the gas from electrons = E_e = (1.169)(0.0282)N

= (1.169)(0.0282)N

= 0.0330N

Energy absorbed in the gas from gammas

= E_g

= 0.0292N

Total energy absorbed in the gas from gammas and electrons

= $E_g + E_e$

= 0.0292N + 0.0330N

= 0.0622N

Energy absorption ratio

= $(E_g + E_e)/E_g$

= 0.0622N/0.0292N

= 2.13

Cobalt 60:

1/S at 10mm = 1.175

Energy absorption coefficient for Al = 0.0258 cm^2/g

Energy absorption coefficient for air = 0.0268 cm^2/g

Energy absorbed in the gas from electrons

= (1.175)(0.0258)N

= 0.0303N

Energy absorbed in the gas from gammas

= 0.0268N

Total energy absorbed in the gas from gammas and electrons

= 0.0268N + 0.0303N

= 0.0571N

Energy absorption ratio

= 0.0571/0.0268N

= 2.13

In these calculations N is a parameter characteristic at the gamma energy and the gas.

The energy absorption ratios calculated above are for mono-directional radiation. If a bi-directional situation is assumed, with gamma radiation perpendicularly incident on each wall, the gamma dose rate in the gas will be doubled, as will the electron dose rate; hence

Energy absorption ratio = $(2\ E_e + 2\ E_g)/2\ E_g = (E_e + E_g)/E_g$

The energy absorption ratio will therefore be independent of the number of directions from which gamma radiation is incident.

The ionization per unit mass of the gas for different wall materials varies across the channel in approximately the same way as for the aluminum wall. However, because the amount of the ionization is proportional to the quotient of mass energy-absorption coefficient for the wall by the mass stopping power ratio of the wall to the gas, higher Z wall materials will produce more ionization per unit mass of the gas, compared to the low Z wall material. But the attenuation of the photons in the wall is high when the atomic number of the wall is high. The contribution of the scattered photons to the ionization must be considered, and, proper correction for scattered photons has to be added to the Spencer-Attix theory.

The ionization for different gases is proportional to gas density divided by the product of the mass stopping power ratio of the wall to the gas times the average energy associated with the formation of one ion pair in the gas.

Over the range of gamma energies of interest the mass stopping power ratio remains nearly constant, but ionization in the gas for a given wall material and lower incident gamma energy will be greater because the mass energy-absorption coefficient at lower gamma energy is greater (E_M will be more and hence ionization in the gas).

If the pressure of the gas is increased, ionization in the gas will be increased because increasing the pressure increases the density of the gas. However, ionization may be reduced at high pressures as a result of ion-pair recombinations.

Discussion

It is clear from the results obtained for the simplified model described earlier that there is definitely an increase in the dose rate imparted to the gas phase. For aluminum as the plate material and air at standard temperature and pressure as a gas, a two-fold increase in absorbed dose rate is predicted for monoenergetic radiation.

Although many designs are available for irradiation with gamma emitting isotopes and the associated shielding, one the most suitable designs for irradiation vs. gases is with the gamma source arranged to irradiate a cavity (generally cylindrical). A gas or mixture of gases to be irradiated circulates through the cavity under suitable conditions of temperature and pressure as shown in the Figure 8. A typical facility is cylindrically concentric with an external annular source as shown in the Figure 8. For the gas phase dose rate improvement, electrons conversion plates will be introduced in the cavity.

The results of the model discussed in this thesis could be extended to the practical case by:

1. Introducing concentric cylinders to proper thickness with proper channel spacing between two consecutive concentric cylinders.
2. By proper packing of the irradiated cavity with the pipes of proper thickness and proper wall separation. The gas will circulate through these pipes.

The case of concentric cylinders approximates the model discussed in this thesis. However, a larger number of conversion

plates could be introduced in the case of packing of the pipes in the cavity. Thus the dose rate will be improved if the cavity is packed with the pipes.

If the pipes have circular cross section, packing of the pipe will leave some empty space as shown in Figure 20. The secondary wall electron escaping into this empty space between these will not be able to impart energy in the gas. This could be improved by letting the gas flow through these empty spaces too.

An alternative way of utilizing energy of all the electrons will be to use hexagonal cross sectional pipes instead of circular pipe because packing of hexagonal pipes will not allow any empty spacing between pipes. The thickness of hexagonal pipes however should be half of the proper thickness because in closed packing the thickness of two adjoinimg wall will be added linearly. (Figure 21)

The experimental evaluation of the increase in the dose rate for a practical case can be done for a particular candidate system. For example, irradiation of air results in the production of ozone. The amount of ozone produced by irradiation of the air could be calculated by the use of mass spectrometer. Therefore, the amount of ozone production with and without the use of electron conversion plates will determine the increase in the dose rate to the gas phase. The nitrous dioxide dosimeter is used for measurement of dose in the range of 50,000 to 90,000 rads for the measurement of the energy absorption in gaseous systems.[34] The nitrous dioxide dosimeter is another candidate system for the experimental evaluation of the increase in the dose rate.

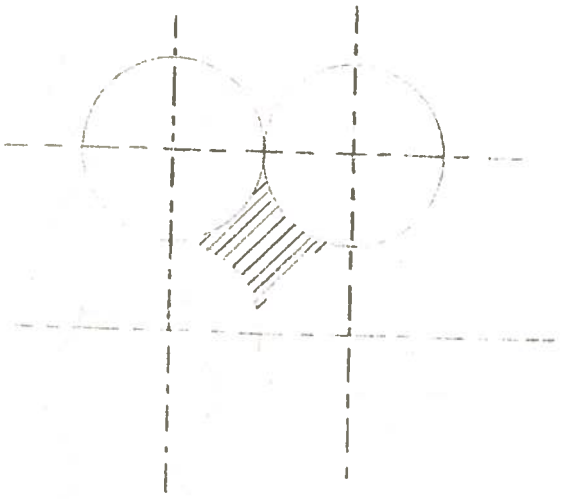

Figure 20: Packing of Circular Cross Sectional Pipes.

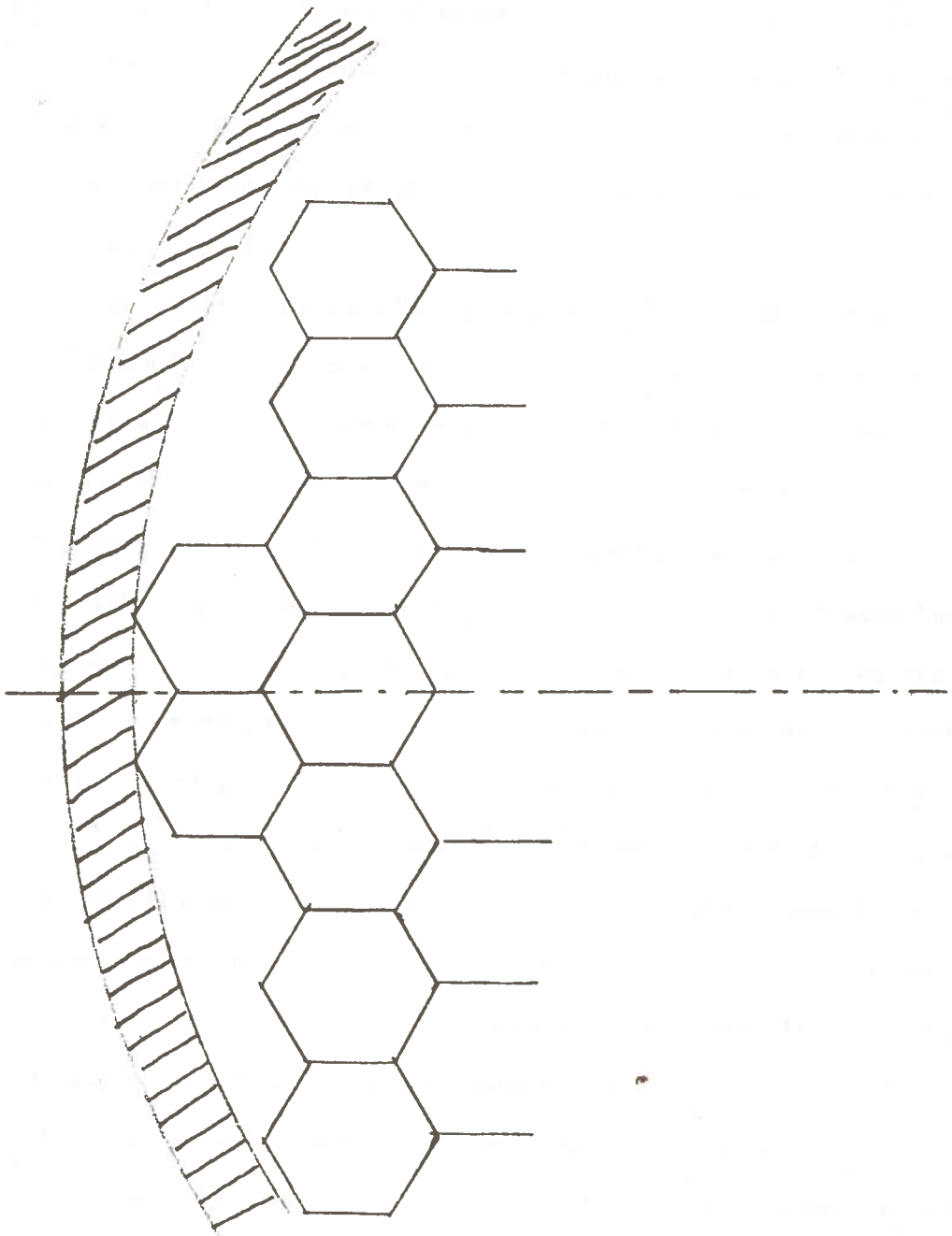

Figure 21: Packing of Hexagonal Cross Sectioal Tubes in a Cylinderical Irradiator.

Theoretical calculations for the stopping power ratio used for the model utilizes table functions provided by the National Bureau of Standards.[35] Values of these table functions are not available for all the materials and in all the energy ranges of the secondary electrons. Further work is recommended to calculate these functions in the main program itself to allow this main program to be more generally applicable.

This model has assumed perpendicularly incident radiation only, which would not be true for a practical irradiation arrangement. Modification of the model to incorporate a line source immediately adjacent to the irradiation vessel, and introduction of a term for radiation backscattered from shielding would allow for a more realistic approximation of a practical case. It would also be necessary to calculate average ionization density over the entire reaction vessel to take into account both vertical and horizontal variation of gamma dose rate. Prediction of the results from a practical irradiator as compared to the results from the simple model is not straightforward. Scattered radiation would lead to an increase in photoelectron contribution, which would suggest an increase in ionization density in the gas; however, the probability of forward scattered electrons would be reduced, suggesting a lower probability of escape from the wall, and also a softer electron spectrum. Intuitively, it would seem that the simple model assumed for this thesis over estimates the dose rate improvement for a real case.

The model does not, however, include calculation of dose rate contribution from (a) secondary electrons ejected backwards from the second wall into the gas, or (b) backscattering of electrons from

the first wall into the gas by the second wall. The latter effect may not be significant, but the backward ejection of electrons may contribute strongly to the gas phase dose rate. This contribution would be expected to be greatest for low energy gamma radiation, which would result from scattered radiation in a practical irradiator. Experimentally observed values may, therefore, be greater than those predicted by the simple model.

CHAPTER V

SUMMARY AND CONCLUSIONS

Irradiation of various gases has been investigated for the possible use in the chemical industry to produce new products. Artificial radioactive isotopes such as cobalt-60 and cesium-137 (both gamma sources) are most commonly used for radiation-chemical studies. Primary interactions of gammas with matter involve the production of secondary electrons. It is the interactions of these electrons with matter that deposit most of the energy to any absorbing material. So in the case of gases it is advantageous to utilize also the secondary electrons produced in the walls of the reaction vessel to increase the energy transfer from gamma to the gas phase. The purpose of this thesis is to calculate theoretically the increase in energy transfer to a gas by electrons produced in plates introduced into the vessel as a function of plate thickness, distance between plates, and atomic number of the plate materials.

The range of an electron in a material is inversely proportional to the density of the material. Therefore, low Z materials will allow a maximum number of electrons to escape from the walls of containers. Aluminum is considered to be a more suitable wall material than other low Z materials (e.g., glass or polyethylene) because there is no gamma radiation damage in metal as compared to other materials.

The gamma sources considered in this thesis are Co-60 (1.25 Mev average energy) and Cs-137 (0.66 Mev) because these sources are most commonly used. Although there are twelve possible interactions of gamma with matter, only photoelectric and Compton interaction are important for gamma sources considered in this paper.

The secondary electrons generated by direct interactions have kinetic energies such that they lose their energy while traveling in the matter mostly by inelastic collisions with atomic electrons. Inelastic collisions with atomic nuclei, which results in Bremsstrachlung emission, is dominant only for the electron energies between 10 and 100 Mev depending on the stopping material. In the case of aluminum, a critical energy, at which energy loss due to electron collisions is equal to loss due to Bremsstrahlung, is approximately 50 Mev. Interaction of electrons with atomic nuclei is therefore neglected for the purpose of this thesis. Elastic collisions with nuclei is important for electron energies in the low Mev range, and elastic collisions with the electron is important only for electrons energy below 100 ev. Hence, elastic collisions in the atomic nuclei and atomic electron are also neglected for the purpose of this paper.

The simplified model discussed in this thesis assumes mono-energetic incident gamma radiation delivered as a collimated beam perpendicular to a single pair of infinite plane parallel plates defining the gas volume. The optimum thickness of the plates should be such that the maximum number of secondary electrons should escape from the plate to interact with the gas. The rate of escape of secondary electrons depend upon the electron spectrum generated in the wall. If the thickness of the plate is just equal to the range of the average energy electron generated in the plate, then the electrons generated in a layer of the wall next to the gas will be able to escape from the wall, while electrons generated in a layer close to the opposite surface of the wall may be just able to reach

the other face and may not escape into the gas. It has been found experimentally that most of the electrons escaping from a plate are generated in a very thin layer of the plate next to the gas.[25] This is due to the reason that when a beam of gamma rays enters a medium the energy lost by the electrons per unit volume at a location near the surface is less than the initial kinetic energy released per unit volume at the same location. The ratio between the two increases with depth, until the ratio of the energy absorbed to that released with in an elementary volume reaches a constant value independent of position along the beam. Therefore, the optimum thickness should be chosen as some fraction of the range of secondary electrons.

In the case of photoelectrons, because the energy of most of the electrons generated is essentially constant, absorption of these electrons will be similar to linear absorption for monoenergetic electrons. However, in the case of Compton electrons the energy distribution could be compared with the continuous energy distribution of a pure beta emitter. The rate of electron escape from the wall will approach a constant value after a certain thickness of absorber. This thickness is "optimum" and is calculated by assuming a linear energy distribution model.

For establishing wall separation, it is necessary to calculate the residual energy of most of the electrons on reaching the surface next to the gas phase from the origin of their production. Then, depending on the range of these electrons in the gas, inter-plate separation could be calculated. But it is not possible to calculate theoretically the residual energy of secondary electrons on reaching

the surface from the origin of their production because of the lack of the cross section values for electrons of low energy. In the case of cavity ionization chambers, the energy absorbed in the wall mater material is calculated by measuring ionization produced in the gas of the cavity. The energy absorbed per unit mass or per unit volume of the wall material is equal to 1/S times the energy absorbed per unit mass or per unit volume by the gas, where S is the mass stopping power ratio calculated by the Spencer-Attix theory. This theory is applied here to calculate stopping power ratios for different channel widths. As energy absorbed per unit mass of the wall material could be calculated from mass energy absorption coefficients of the material at given gamma energy, we could calculate theoretically the ionization produced per unit mass of the gas, from the stopping power ratio and from the energy disspitated per ion pair formed in the gas, W.

It is important to calculate stopping power ratio as accurately as possible. Although there are various theories developed to calculate stopping power ratios the Spencer-Attix theory is very close to experimental values.[29] Moreover, this theory takes into account the effect of fast electrons, generated by the interaction of secondary electrons with the atomic electfons. Some of these electrons will escape into the gas.

Let Δ be this energy needed by an electron to be able to just cross the wall separation before stopping. Electrons with an energy less than Δ are assumed to dissipate their energy on the spot where they originate. The Spencer-Attix theory is to be applicable for $\Delta \ll T_o$, T_o being the average energy of the secondary electrons

generated by the gamma interaction with the wall material. Selection of different values of Δ really means different wall separations, because the range in gas of electrons with energy Δ is equal to the wall separation. The calculations of stopping power ratios requires the use of the table functions provided by the National Bureau of Standards. These calculations are done for aluminum and for Co-60 and Cs-137 gamma sources with the help of a computer program.

From the plots of ionization per unit mass of the gas as a function of wall separation, proper wall separation is chosen. The wall separation is considered to be that distance at which ionization per unit mass of the gas is almost constant.

Based upon this simplified model, using aluminum as the wall material and air at standard conditions on the gas, the selected wall thickness and channel width are, respectively, 0.45mm and 10mm for Cobalt-60, and 0.13mm and 10mm for cesium-137. In both cases the ratio of electrons plus gamma does rate to the gamma does rate only is 2.13 for monodirectional radiation. This ratio will remain the same for multidirectional irradiation.

In the practical case of polydirectional gamma source and cylinderical irradiation chamber, does rate improvement can be achieved by introducing concentric cylinders of proper wall thickness and proper wall separation (distance between two consecutive cylinders). The gas phase does rate can further be improved by increasing the number of walls, which can be accomplished by packing the cavity with square or hexagonal cross-section pipes to provide uniform channel geometry.

Further work is recommended for experimental evaluation of the increase in gas phase dose rate by the use of electrons conversion plates for a practical case. The suggested candidate systems can be the measurement of ozone produced by irradiation of air, or the nitrous dioxide dosimeter for measurement of gas phase dose rate.

REFERENCES

1. K. Yang and P. L. Gant, Journal of Physical Chemistry, Vol.65, p.77, 1961.

2. D. A. Armstrong and J. W. Spinks, Canadian Journal of Chemistry, Vol. 37, p.1210, 1959.

3. G. L. Brownell, F. J. Mahoney, J. J. Fitzgerald, Mathematical Theory of Radiation Dosimetry, Gordon and Breach Science Publishers, Inc., New York, 1967.

4. J. Weiss, "Chemical Dosimetry Using Ferrous and Ceric Sulfates" Nucleonics, July 1952, p.28.

5. W. J. McGonnagle, "Non-Destructive Testing", Gordon and Breach Science Publishers, Inc., New York, 1969.

6. R. D. Evans, "The Atomic Nucleus", McGraw-Hill Book Company, Inc., New York, p.695.

7. Ibid., p.712.

8. Ibid., p.712.

9. White-Gordstein, "National Bureau of Standards", (U.S.), Circulation 5-83, 1957.

10. C. M. Davisson and R. D. Evans, "Revised Modern Physics", Chapter 23, 1955.

11. F. A. Attix and W. R. Roesch, "Radiation Dosimetry", Vol. 1, Academic Press, New York, 1968.

12. Ibid., p.102.

13. A. T. Nelms, "National Bureau of Standards", (U.S.), Circulation 542, 1953.

14. Reference 11, p.143.

15. Reference 6, p.691.

16. Ibid., p.693.

17. G. J. Hine and G. L. Brownell, "Radiation Dosimetry", Academic Press, Inc., New York, 1950.

18. R. P. Gardner and R. L. Ely, Jr., "Radiation Measurements Applications in Engineering", Reinhold Publishing Corporation, New York.

19. J. D. Jackson, "Classical Electrodynamics" Wiley Publishing Company, New York, 1962.

20. Reference 11, p.175.

21. RSIC Computer Code Collection CCC-127, Oak Ridge National Laboratory,U. S. Atomic Energy Commission. (MORSE)

22. L. H. Gray, "Proceeding of Royal Society", Vol.A156, p.578, 1936.

23. Reference 6, p.563.

24. L. K. Katz and A. S. Penfold, "Review of Modern Physics", Vol. 24, p.28, 1952.

25. L. H. Gray, "Radiation Dosimetry", British Journal of Radiology, Vol. 10, p.600-721, 1937.

26. Check and Linnenbom, B. J., U. S. Naval Research Laboratory, January 1958.

27. Reference 1, Chapter IV.

28. "Effect Des Parois En Vere Dans La Dosimetrie Au Sulfate Ferreux", J. R. Puigh and J. Sutton. Journal De Chimie Physicque, Vol. 56, p.699, July 1959.

29. G. N. Whyte, "Measurement of the Brass-Gray Power Correction", Radiation Research, Vol. 6, p.371, 1957.

30. G. C. Laurence, Canadian Journal of Research, Vol. 5, p.558, 1937.

31. L. V. Spencer and F. H. Attix, "Radiation Research", Vol. 3, p.239, 1955.

32. L. V. Spencer, W. Fano, "Energy Spectrum Resulting from Electron Slowing Down", Physics Review, Vol.93, p.1172, 1954.

33. "Stopping Powers for use with Cavity Chambers", National Bureau of Standards Handbook 79, Sept. 1961.

34. P. H. Azteck and S. Dondes, Nucleonics, Vol. 14, p.66, 1956.

35. Reference 33, pp. 43-45.

36. Ralph E. Lapp, and Howard L. Andrews, "Nuclear Radiation Physics", p.153, Prentice-Hall, Inc., Englewood Cliffs, NJ.

APPENDIX A

Computer Program and Flow Diagram

Instructions to use Computer Program:

The following input information is necessary for use of the computer program.

1. First card should have the value of the energy of the gamma source and the value of the linear coefficient for photoelectric interaction in the units of Mev and $(\text{centimeter})^{-1}$ respectively. The format for these two values is F6.4.
2. Second card should have the values of the atomic number, atomic weight of the wall material, atomic number, atomic weight of the gas, the ionization potential of the gas and wall material (in the units of electron volts). The respective format for this information is F12.6.
3. Third card should have the values of range in the gas corresponding to electrons of energy 2.56, 5.12, 10.24, 20.48, 40.96 and 81.82 Kev respectively. The format for this information is F7.3.
4. Fourth card should have the value of the classical radius of the electron in the units of centimeter and the value of the number of electrons per cubic centimeter of the material in the respective "Format" of E11.4 and E10.3.
5. Next input cards have the values of the table functions B_z, D_z, A_z, d_z and c_z as provided in Appendix B. These functions are stored as two dimentional arrays $X_1(I,J)$, $X_2(I,J)$, $X_3(I,J)$ $X_4(I,J)$ and $X_5(I,J)$ respectively in "Format" of 11F7.5.

This program is good for only a few wall materials, i.e., aluminum, carbon, copper, tin and lead because of the limited information of the values of the table functions.

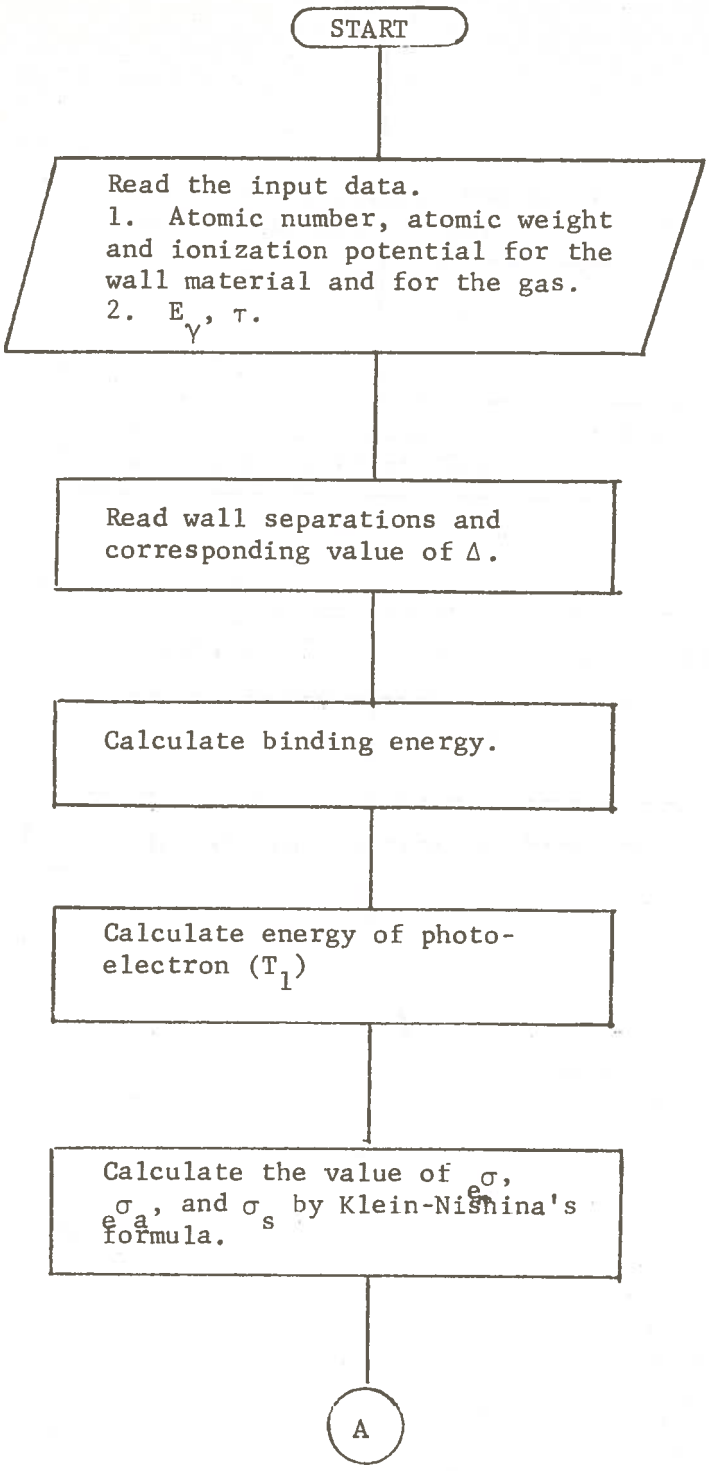
START
Read the input data.
1. Atomic number, atomic weight and ionization potential for the wall material and for the gas.
2. E_γ, τ.
Read wall separations and corresponding value of Δ.
Calculate binding energy.
Calculate energy of photo-electron (T_1)
Calculate the value of σ_e, σ_a, and σ_s by Klein-Nishina's formula.
A

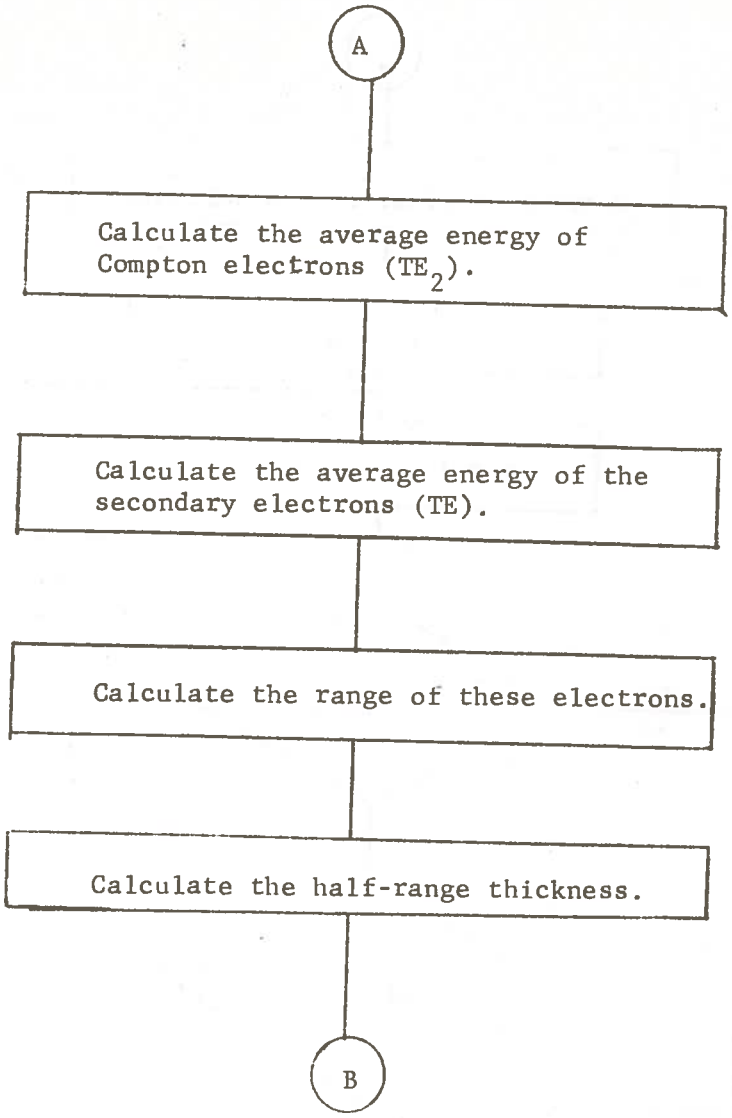
A
Calculate the average energy of Compton electrons (TE_2).
Calculate the average energy of the secondary electrons (TE).
Calculate the range of these electrons.
Calculate the half-range thickness.
B

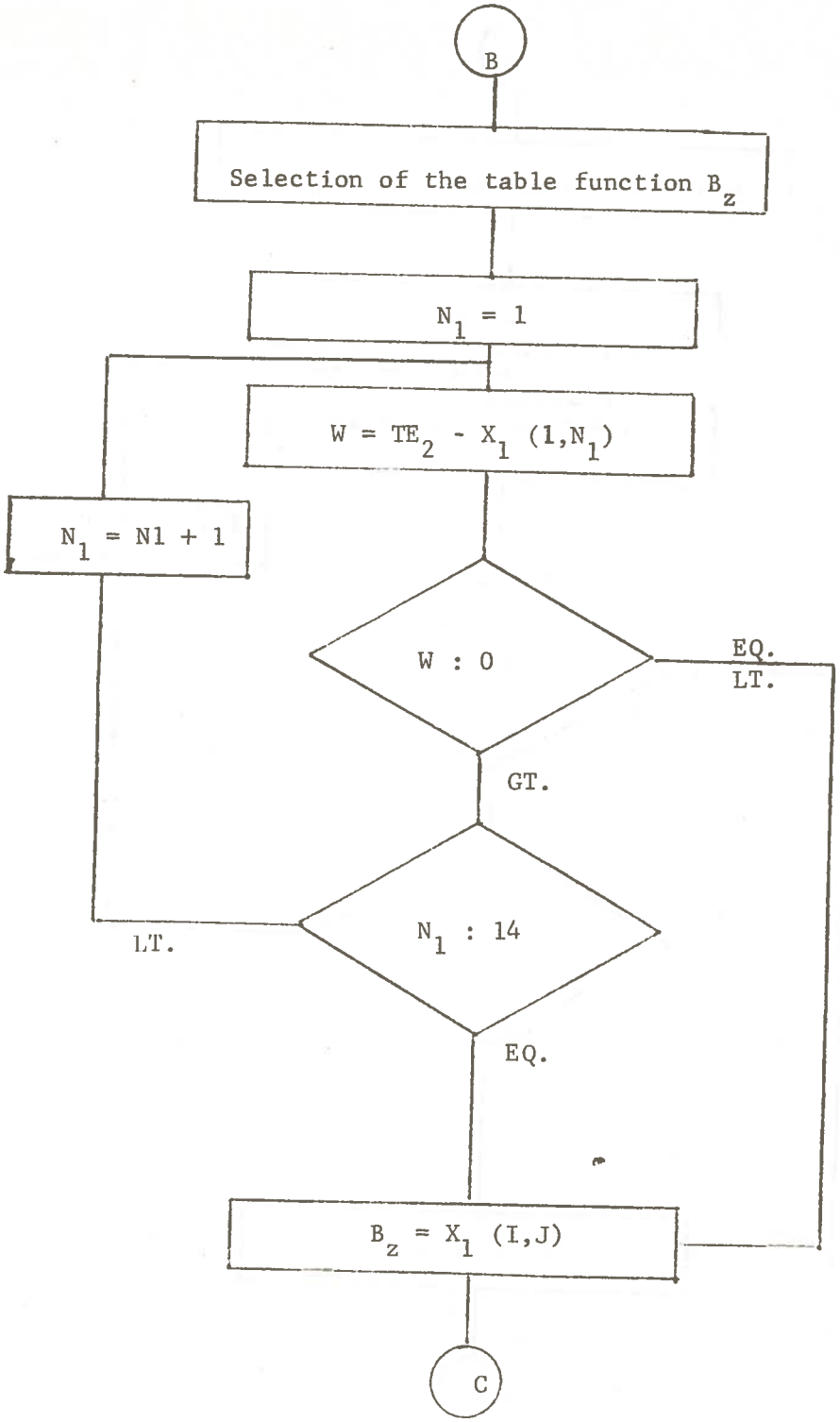
B
Selection of the table function B_z
$N_1 = 1$
$W = TE_2 - X_1 (1,N_1)$
$N_1 = N1 + 1$
W : 0
EQ.
LT.
GT.
N_1 : 14
LT.
EQ.
$B_z = X_1 (I,J)$
C

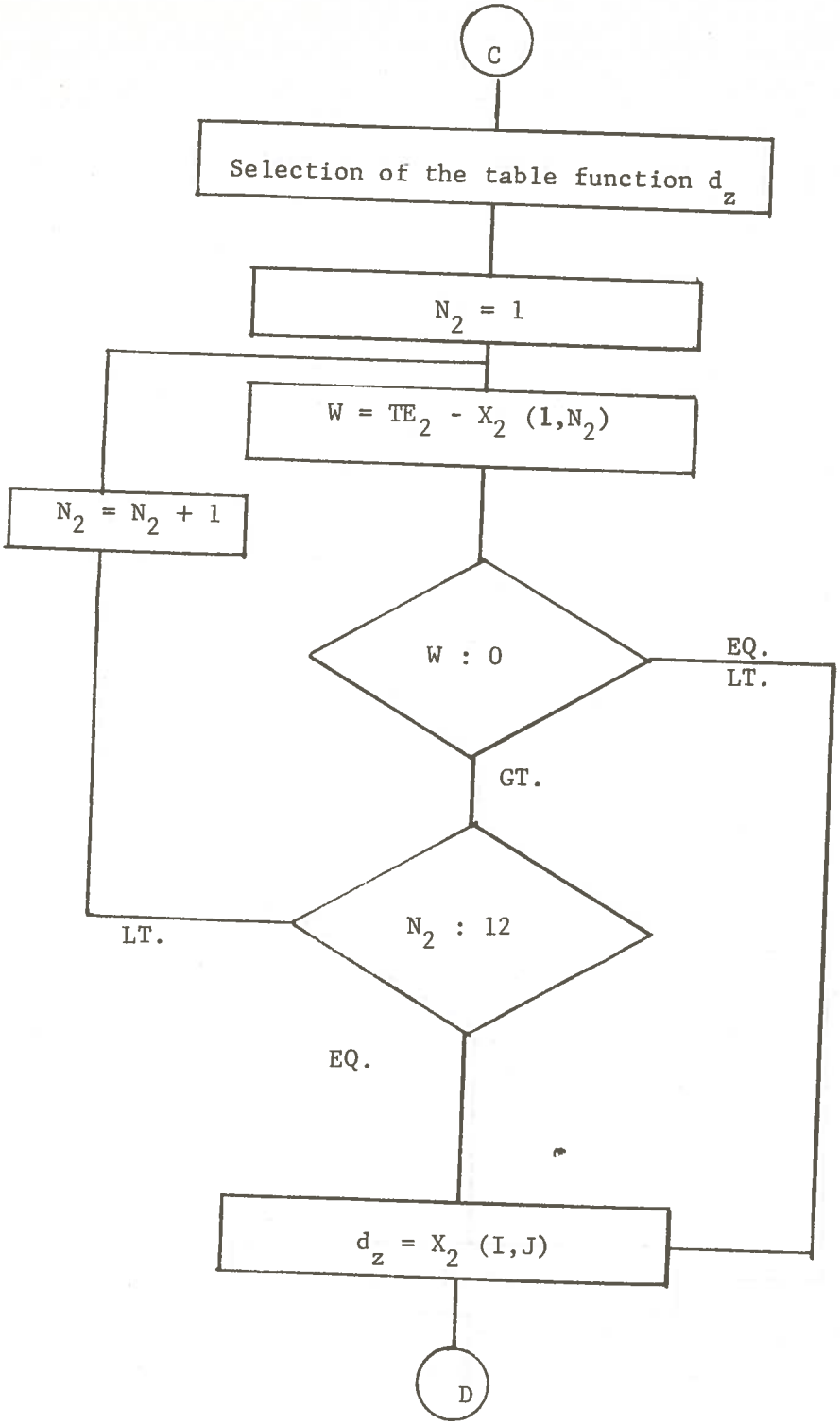
C
Selection of the table function d_z
$N_2 = 1$
$W = TE_2 - X_2 (1,N_2)$
$N_2 = N_2 + 1$
W : 0
EQ.
LT.
GT.
N_2 : 12
LT.
EQ.
$d_z = X_2 (I,J)$
D

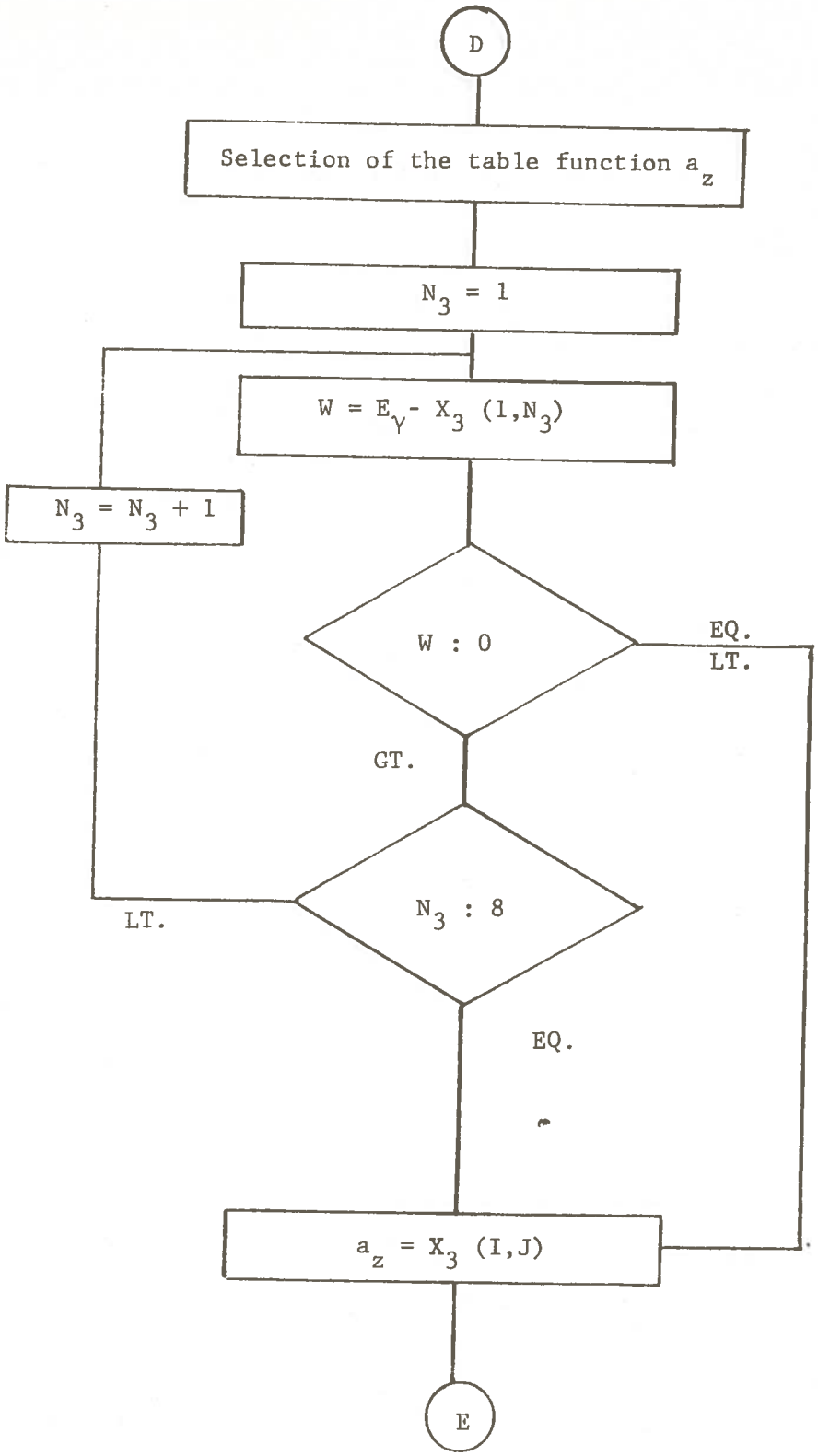
D
Selection of the table function a_z
$N_3 = 1$
$W = E_\gamma - X_3 (1,N_3)$
$N_3 = N_3 + 1$
W : 0
EQ.
LT.
GT.
N_3 : 8
LT.
EQ.
$a_z = X_3 (I,J)$
E

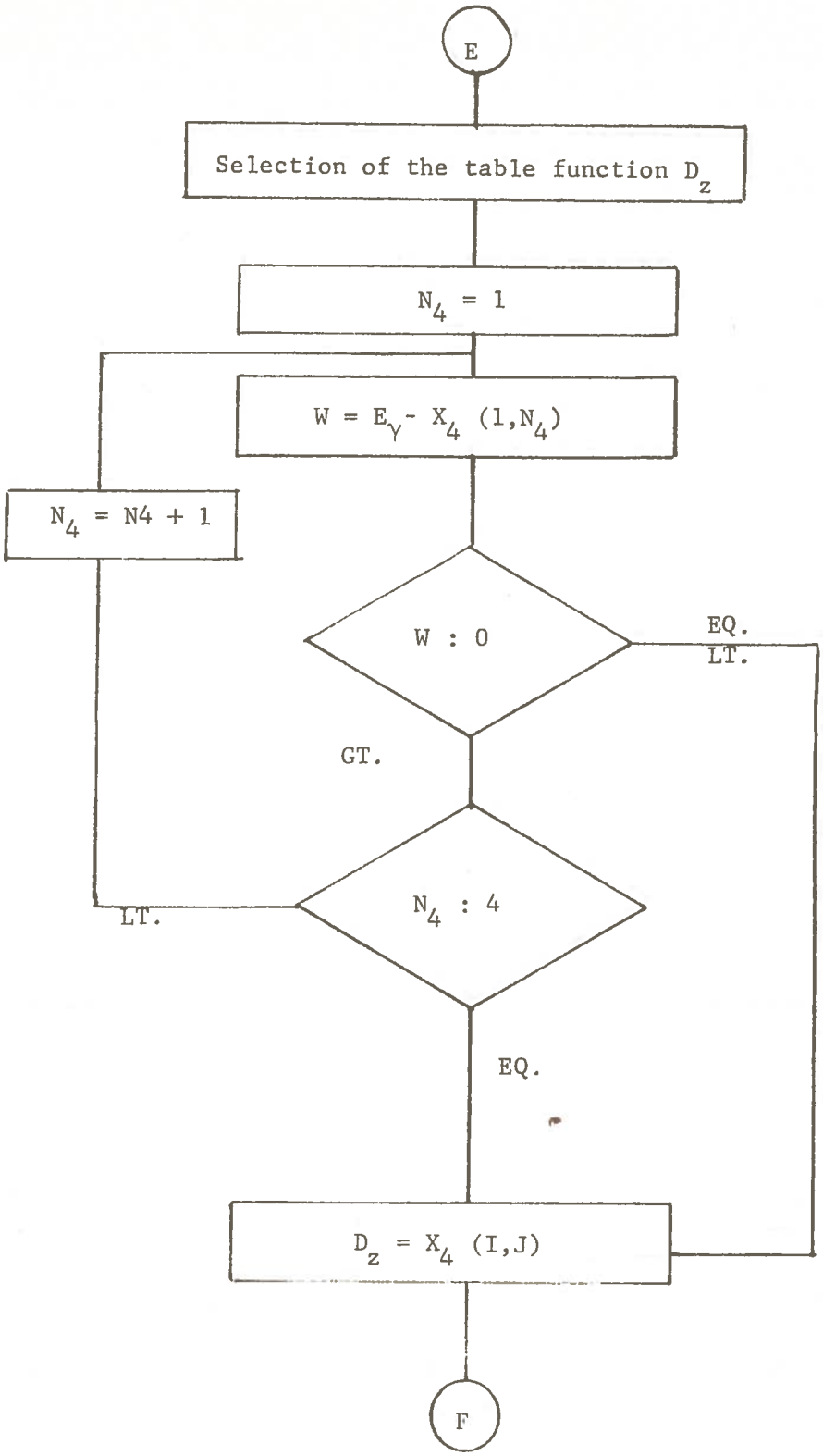
E
Selection of the table function D_z
$N_4 = 1$
$W = E_\gamma - X_4 (1,N_4)$
$N_4 = N4 + 1$
W : 0
EQ.
LT.
GT.
N_4 : 4
LT.
EQ.
$D_z = X_4 (I,J)$
F

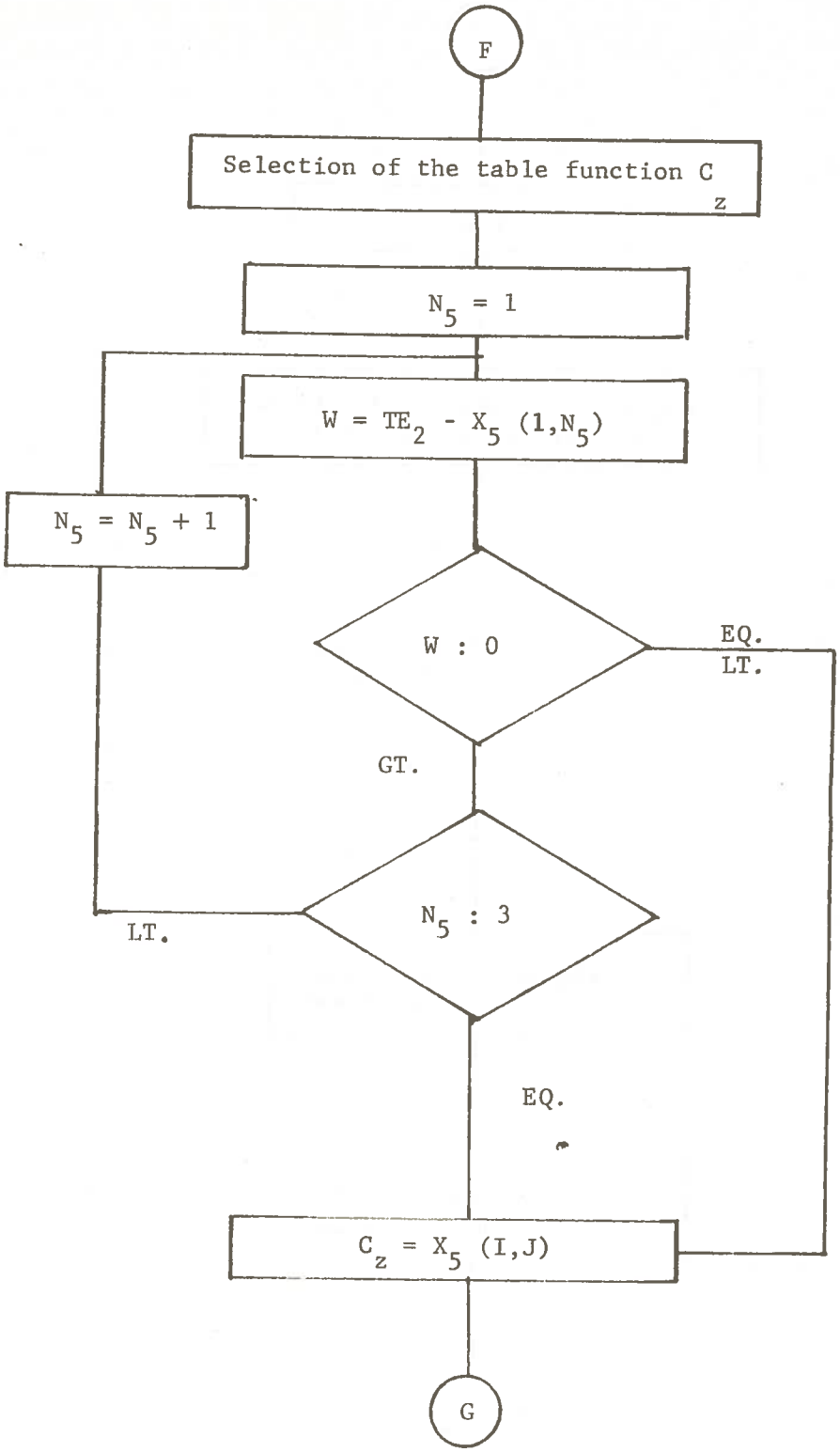
F
Selection of the table function C z
$N_5 = 1$
$W = TE_2 - X_5 (1,N_5)$
$N_5 = N_5 + 1$
W : 0
EQ.
LT.
GT.
N_5 : 3
LT.
EQ.
$C_z = X_5 (I,J)$
G

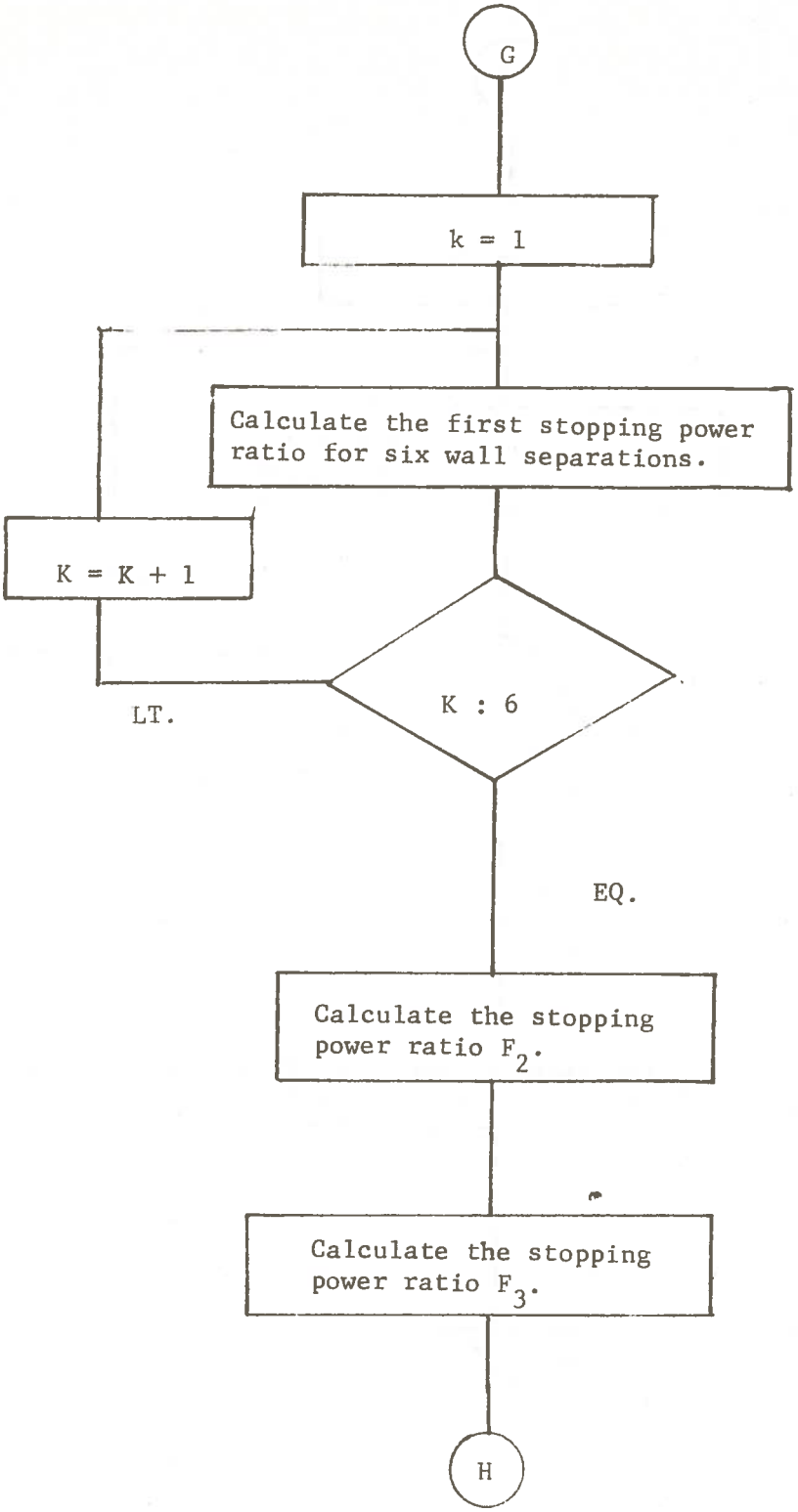
G
k = 1
Calculate the first stopping power ratio for six wall separations.
K = K + 1
K : 6
LT.
EQ.
Calculate the stopping power ratio F_2.
Calculate the stopping power ratio F_3.
H

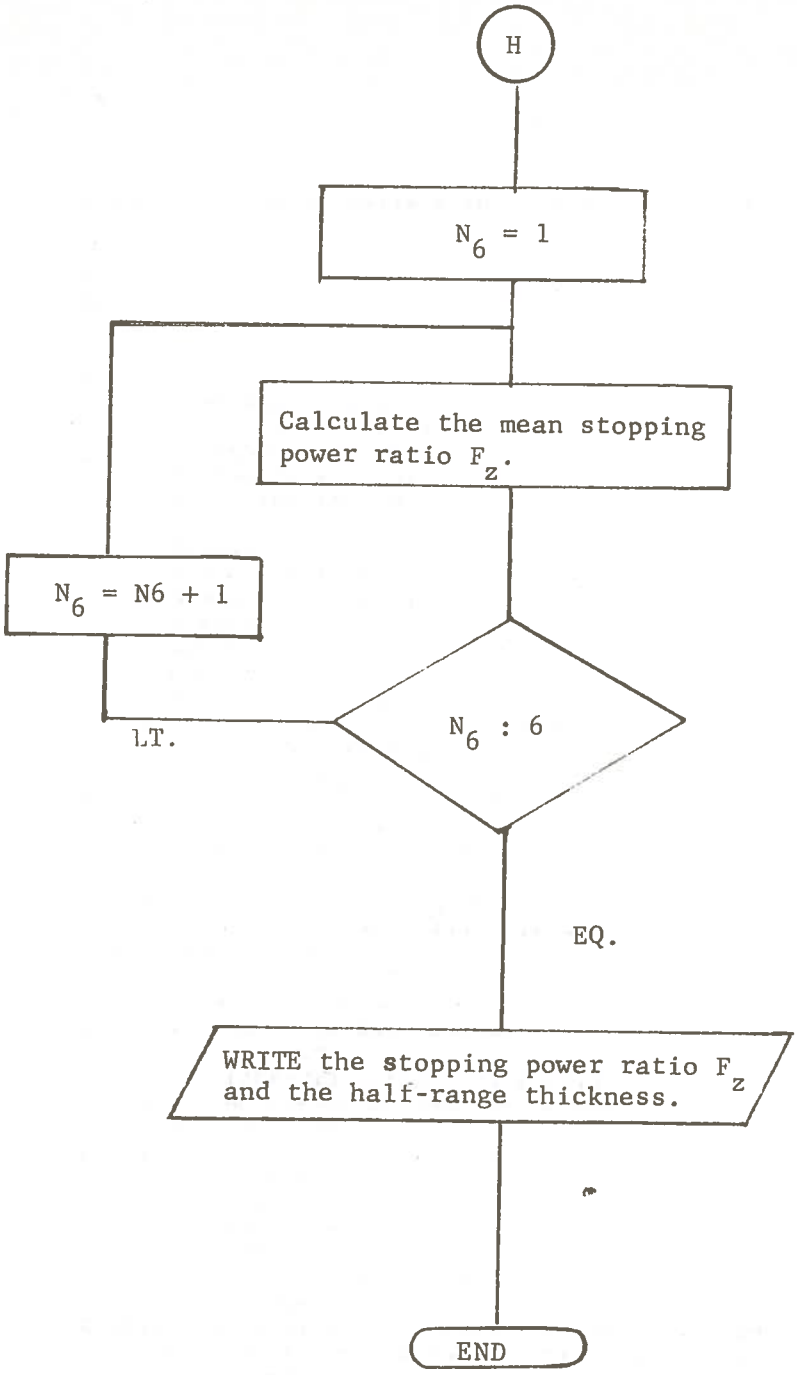
H
$N_6 = 1$
Calculate the mean stopping power ratio F_z.
$N_6 = N6 + 1$
$N_6 : 6$
LT.
EQ.
WRITE the stopping power ratio F_z and the half-range thickness.
END

```
C CALCULATIONS OF OPTIMUM THICKNESS AND STOPPING POWER RATIO
C
C
C
C
C
C
C
      DIMENSION X1(2,14)
      DIMENSION X2(2,12)
      DIMENSION X3(2,8)
      DIMENSION X4(2,4)
      DIMENSION X5(7,3)
      DIMENSION CZ(6)
      DIMENSION  RP1(6)
      DIMENSION F1(6)
      DIMENSION   FZ(6)
      DIMENSION  WALL(6)
      READ(5,702) NDATA
  702 FORMAT(I3)
      DO 701 MM=1,NDATA
C TGAM IS THE ENERGY OF GAMMA SOURCE
      READ(5,2) TGAM,TAU
    2 FORMAT(F6.4,F6.4)
C ZZ AND XZ ARE  ATOMIC  NO AND ATOMIC WEIGHT OF WALL MATERIAL
C     AG AND ZG ARE ATOMIC NO AND ATOMIC WEIGHT OF THE GAS
      READ(5,28) ZZ,XZ,ZG,AG,FIG,FIZ
   28 FORMAT(6F12.6)
C    WALL(II) IS  WALL  SEPARATION
      READ(5,700) (WALL(II) ,II=1,6)
  700 FORMAT(6F7.3)
      READ(5,1)   RZERO,FNZ
    1 FORMAT(      E11.4,E10.3     )
C CALCUTIONS OF BINDING ENERGY
      ZEFF=ZZ-0.3
      BE=((ZEFF/137.)**2)/(0.511/2.)
C TE1 IS THE ENERGY OF PHOTO-ELECTRON
      TE1 =TGAM-BE
C CALCULATIONS OF ESIGMA BY KLEIN-NISHINA FORMULA
      A=TGAM/0.511
      G1=A+1.
      G2=(G1 )/(A**2)
      G3=2.*A+1.
      G4=2.*3.142*(RZERO**2.)
      G5=1.+(3.*A)
C ESIGM IS COLLISION DIFFERENTIAL CROSS SECTION
      ESIGM=G4*(G2*(((2.*G1)/G3)-((ALOG(G3))/A))+((ALOG(G3))/(2.*A))-
     1(G5/(G3**2)))
      G6=(2.*(A**2))-(2.*A)-1.
      G8=G6*2.*G1
      G9=ALOG(G3)
```

```
      G10=G9/(A**3.)
      G13=A**2.
      G14=G3**2.
      G11=G8/(G13*G14)
      G12=8.*G13/(3.*(G3**3))
      ESIGMS=(G4/2.)*(G10+G11+G12)
      ESIGMA=ESIGM-ESIGMS
      TE2=(TGAM*ESIGMA)/ESIGM
      SIGMA=FNZ*ESIGM
      FMU=TAU+SIGMA
C TE  IS THE AVERAGE ENERGY OF ALL THE SECONDARY ELECTRONS
      TE=((TE1*TAU)/FMU)+((TE2*SIGMA)/FMU)
      G20=1.265-(.0954*ALOG(TE ))
C RANGE AND THICKNESS CALCULATIONS
C GR IS THE RANGE OF THE AVERAGE ENERGY SECONDARY ELECTRONS IN THE METAL
      GR=412.*((TE )**G20)
C TH IS THE THICKNESS ( OPTIMUM  )
      TH=GR/(2.3*1000.*2.)
      WRITE(6,600) TGAM,TH
  600 FORMAT(/30X,'ALUMINUM AND GAMMA ENERGY OF',F5.3//8X,'OPTIMUM THICK
     *NESS IN CM.==',E15.5)
      WRITE(6,705)
  705 FORMAT(/12X,'WALL SEPARATION',20X,'STOPPING POWER RATIO')
C  THE  EVALUATION  OF  TABLE  FUNCTIONS
C   X1(I,J) IS  THE  FUNCTION BZ FOR  ALUMINUM
      READ(5,3) ((X1(I,J),J=1,14),I=1,2)
    3 FORMAT(11F7.5)
      DO 4 N1= 1,14
      W1=TE2-X1(1,N1)
      IF(W1) 5,5,4
    4 CONTINUE
    5 M1=N1-1
      IF(M1.EQ.0) GO TO 399
      Y1=ABS(TE2-X1(1,M1))
      IF(W1.GT.Y1) GO TO 6
  399 BZ=X1(2,N1)
      GO TO 7
    6 BZ=X1(2,M1)
    7 CONTINUE
C X2(I,J) IS  THE FUNTION DZ
      READ(5,8) ((X2(I,J),J=1,12),I=1,2)
    8 FORMAT(11F7.5)
      DO 9 N2 = 1,12
      W2=TE2-X2(1,N2)
      IF(W2) 10,10,9
    9 CONTINUE
   10 M2=N2-1
      IF(M2.EQ.0) GO TO 400
      Y2=ABS(TE2-X2(1,M2))
      IF(W2.GT.Y2) GO TO 11
```

```
  400 SDZ=X2(2,N2)
      GO TO 12
   11 SDZ=X2(2,M2)
  12  CONTINUE
C X3(I,J) IS THE FUNCTION AZ
      READ(5,13) ((X3(I,J),J=1,8),I=1,2)
   13 FORMAT(11F7.5)
      DO 14 N3=1,8
      W3=TGAM-X3(1,N3)
       IF(W3) 15,15,14
   14 CONTINUE
   15 M3=N3-1
      IF(M3.EQ.0) GO TO 401
      Y3=ABS(TGAM-X3(1,M3))
      IF(W3.GT.Y3) GO TO 16
  401 AZ=X3(2,N3)
      GO TO 17
   16 AZ=X3(2,M3)
   17 CONTINJE
C  X4(I,J) IS THE FUNCTION  DZ
      READ(5,18) ((X4(I,J),J=1,4),I=1,2)
   18 FORMAT(8F7.5)
      DO 19 N4 = 1,4
      W4 =TGAM-X4(1,N4)
      IF(W4) 20,20,19
   19 CONTINUE
   20 M4=N4-1
      IF(M4.EQ.0) GO TO 402
      Y4=ABS(TGAM-X4(1,M4))
      IF(W4.GT.Y4) GO TO 21
  402 DZ=X4(2,N4)
      GO TO 22
   21 DZ=X4(2,M4)
   22 CONTINUE
C  X5(I,J) IS THE FUNCTION  CZ( DEL,  T)
      READ(5,23) ((X5(I,J),J=1,3),I=1,7)
   23 FORMAT(11F7.5)
      DO 24 N5 =1,3
      W5=TE2-X5(1,N5)
      IF(W5) 25,25,24
   24 CONTINUE
   25 M5=N5-1
      IF(M5.EQ.0) GO TO 403
      Y5=ABS(TE2-X5(1,M5))
      IF(W5.GT.Y5) GO TO 27
  403 DO 45 L=1,6
      LI=L+1
      CZ(L)=X5(LI,N5)
   45 CONTINUE
      GO TO 47
```

```
   27 DO 46 K= 1,6
      KI=KI+1
      CZ(K)=K5(KI,MS)
   46 CONTINUE
   47 R=FIZ/FIG
      Q=(ZG/AG)/(ZZ/XZ)
      G7=ALOG (R)
      LM=1
      DO 30 N6 =1,6
      RP1(N6)=Q*(1+CZ(LM)*(ALOG(R)+SDZ))
      F1(N6)=1/RP1(N6)
      RP2=Q*(1+(BZ*(ALOG(R)+SDZ)))
      F2=1/RP2
      RP3=Q*(1.+(AZ*G7)+DZ)
      F3=1/RP3
C FZ(N6)  IS  THE  MASS  STOPING POWER RATIO FOR DIFF. WALL SEPARATIONS
      FZ(N6)=(F1(N6)*F3)/F2
      WRITE(6,509) WALL(N6),FZ(N6)
  509 FORMAT(/17X,F7.3,25X,E15.5)
   30 LM=LM+1
  701 CONTINJE
      STOP
```

ALUMINUM AND GAMMA ENERGY OF0.662

OPTIMUM THICKNESS IN CM.== 0.13118E-01

WALL SEPARATION	STOPPING POWER RATIO
73.000	0.87032E+00
22.000	0.86235E+00
6.400	0.85268E+00
1.900	0.84220E+00
0.510	0.82846E+00
0.150	0.81107E+00

ALUMINUM AND GAMMA ENERGY OF1.250

OPTIMUM THICKNESS IN CM.== 0.44560E-01

WALL SEPARATION	STOPPING POWER RATIO
73.000	0.86898E+00
22.000	0.86118E+00
6.400	0.85290E+00
1.900	0.84214E+00
0.510	0.82927E+00
0.150	0.81223E+00

APPENDIX B

Function tables required for computer program.

(National Bureau of Standards Handbook 79, pp.43-45)

TABLE B-1

The Function $b_z(T_o)$

T_o(MeV)	C	Al	Cu	Sn	Pb
0.100	0.16430	0.18772	0.22408	0.28880	0.30712
0.200	0.14764	0.16600	0.19262	0.23148	0.24916
0.300	0.13938	0.15544	0.17812	0.20786	0.22408
0.327	0.13780	0.15346	0.17540	0.20320	0.21936
0.400	0.13404	0.14862	0.16908	0.19388	0.20896
0.500	0.13020	0.14366	0.16264	0.18424	0.19836
0.600	0.12722	0.13980	0.15774	0.17702	0.19048
0.654	0.12598	0.13832	0.15570	0.17380	0.18706
0.700	0.12480	0.13664	0.15380	0.17132	0.18424
0.800	0.12278	0.13396	0.15054	0.16666	0.17912
1.000	0.11956	0.12968	0.14536	0.15940	0.17104
1.200	0.11704	0.12634	0.14136	0.15392	0.16490
1.308	0.11580	0.12478	0.13940	0.15120	0.16204
1.500	0.11410	0.12246	--	0.14764	0.15790

TABLE B-2

The Function $d_z(T_o)$

T_o(MeV)	C	A1
0.300	0.00115	0.00006
0.327	0.00154	0.00013
0.400	0.00272	0.00051
0.500	0.00439	0.00120
0.600	0.00606	0.00203
0.654	0.00696	0.00253
0.700	0.00770	0.00291
0.800	0.00930	0.00397
1.000	0.01240	0.00597
1.100	0.01391	0.00693
1.200	0.01537	0.00790
1.308	0.01692	0.00891

TABLE B-3

The Function $a_z(T_e)$

T_e (MeV)	C	Al	Cu	Sn	Pb
0.15	0.20020	0.23796	0.30636	0.46582	0.48180
0.25	0.17318	0.20012	0.24436	0.33174	0.34982
0.4	0.15450	0.17552	0.20650	0.25848	0.27864
0.6	0.14210	0.15904	0.18360	0.21852	0.23478
1.0	0.12948	0.14272	0.16184	0.18396	0.19780
1.5	0.12166	0.13240	0.14894	0.16496	0.17702
2.0	0.11672	0.12592	--	--	--
2.5	0.11334	0.12150	--	--	--

TABLE B-4

The Function $D_Z(T_e)$

T_e (MeV)	C	Al
0.4	0.00014	0.000
0.6	0.00148	0.00022
1.0	0.00597	0.00219
1.5	0.01167	0.00567

TABLE B-5

The Function $c_Z(T_o,\Delta)$

T_o(MeV)	Δ(keV)	C	Al	Cu	Sn	Pb
1.308	81.8	0.12360	0.13372	0.14958	0.16032	0.17416
	40.9	0.12956	0.14110	0.15896	0.17168	0.18812
	20.4	0.13716	0.15058	0.17130	0.18668	0.20682
	10.2	0.14594	0.16192	0.18660	0.20614	0.23260
	5.1	0.15706	0.17662	0.20764	0.23402	0.27172
	2.56	0.17046	0.19468	0.23744	0.27664	--
0.654	81.8	0.12806	0.14014	0.15674	0.16930	0.18512
	40.9	0.13510	0.14876	0.16782	0.18346	0.20124
	20.4	0.14242	0.15810	0.18018	0.19776	0.22062
	10.2	0.15200	0.17050	0.19688	0.21896	0.24838
	5.1	0.16332	0.18576	0.21910	0.24852	0.28914
	2.56	0.17772	0.20670	0.25118	0.29454	--
0.327	81.8	0.13282	0.14672	0.16460	0.17850	0.19594
	40.9	0.14006	0.15560	0.17596	0.19262	0.21284
	20.4	0.14874	0.16660	0.19040	0.21028	0.23510
	10.2	0.15796	0.17880	0.20738	0.23196	0.26382
	5.1	0.17018	0.19526	0.23128	0.26390	0.30866
	2.56	0.18530	0.21690	0.26512	0.31244	--

VITA

Sudesh K. Mahajan was born in Punjab, India on September 23, 1946. His secondary education was obtained in Jullundur (India) S.D.A.S. School from which he graduated in 1965. He received a Bachelor of Science in Mechanical Engineering from Kurukshetra University (India) in May 1970.

After working for a year for Escorts Tractor Company of India, in January 1972 he enrolled in the Graduate School of Louisiana State University. At present he is a candidate for a degree of Master of Science in the Department of Nuclear Engineering.